

# Quantum nonlinear resonance and quantum chaos in Aharonov-Bohm oscillations in mesoscopic semiconductor rings

Gennady P. Berman

*Theoretical Division and Center for Nonlinear Studies, Los Alamos National Laboratory, Los Alamos, New Mexico 87545*

Evgeny N. Bulgakov

*Kirensky Institute of Physics, 660036, Krasnoyarsk, Russia*

David K. Campbell

*Department of Physics, University of Illinois at Urbana-Champaign, 1110 West Green Street, Urbana, Illinois 61801-3080*

Ilya V. Krive

*Institute for Low Temperature Physics and Engineering, Ukrainian Academy of Sciences, 310164, Kharkov, Ukraine*

(Received 10 December 1996)

We consider Aharonov-Bohm oscillations in a mesoscopic semiconductor ring threaded by both a constant magnetic flux and a time-dependent, resonant magnetic field with one or two frequencies. Working in the ballistic regime, we establish that the theory of “quantum nonlinear resonance” applies, and thus that this system represents a possible solid-state realization of “quantum nonlinear resonance” and “quantum chaos.” In particular, we investigate the behavior of the time-averaged electron energy at zero temperature in the regimes of (i) an isolated quantum nonlinear resonance and (ii) the transition to quantum chaos, when two quantum nonlinear resonances overlap. The time-averaged energy exhibits sharp resonant behavior as a function of the applied constant magnetic flux, and has a staircase dependence on the amplitude of the external time-dependent field. In the chaotic regime, the resonant behavior exhibits complex structure as a function of flux and frequency. We compare and contrast the quantum chaos expected in these mesoscopic “solid-state atoms” with that observed in Rydberg atoms in microwave fields, and discuss the prospects for experimental observation of the effects we predict. [S0163-1829(97)09539-8]

## I. INTRODUCTION

Over the past two decades, advances in nanoscale fabrication, experimental techniques, and theoretical understanding have produced whole new classes of mesoscopic systems in which the consequences of the Aharonov-Bohm (AB) effect<sup>1</sup> can be observed and interpreted. Although they differ widely in many respects, the common crucial feature of these systems is that their characteristic linear dimension  $L$  is smaller than the length  $L_\phi$  over which the electron wave function maintains its phase coherence, so that the quantum interference that underlies the AB effect is not destroyed. In this limit, both the transport (non-equilibrium) (Ref. 2) and thermodynamic (equilibrium) (Ref. 3) properties of the non-simply connected mesoscopic systems are periodic functions of the (constant) AB flux  $\Phi$  [and hence, for fixed geometry, of the (constant) applied magnetic field] with period  $\Phi_0 = 2\pi\hbar c/e$ , where  $e$  is the electron charge,  $\hbar$  is the Planck constant, and  $c$  is the velocity of light. The amplitude of the periodic oscillations is a decreasing function of the system size, and vanishes in the thermodynamic ( $L \rightarrow \infty$ ) limit.<sup>2-6</sup> For instance, in an idealized strictly one-dimensional (1D) ballistic ring of length  $L$ , the ground-state energy  $E_0(\Phi)$  will exhibit oscillations of period  $\Phi_0$  with an amplitude of order  $2\pi\hbar v_F/L$ , where  $v_F$  is the Fermi velocity. The flux dependence of the ground state energy (or the corresponding

flux dependence of the free energy,  $F$ , at finite temperature) leads, via the relation  $I_0(\Phi) = -c\partial E_0/\partial\Phi$  [or  $I(\Phi) = -c\partial F/\partial\Phi$  at finite temperature], to a persistent current of order  $I_0 \sim ev_F/L$ .

Persistent currents have been observed experimentally in both metallic<sup>7,8</sup> and semiconducting<sup>9</sup> (quasi)-1D rings. In the case of metallic rings, the (relatively) large number of impurities means that the effects of disorder must be included, and ballistic transport is not expected. Further, because of the relatively large value of  $k_F$  for metals, even thin metallic loops contain many (transverse) channels ( $n \sim Wk_F$ , where  $W$  is the width of the loop), and coupling among these channels means that the strictly 1D approaches cannot be applied.<sup>10</sup> In contrast, in semiconductors the relatively high purity of the materials and the relatively low value of  $k_F$  (which renders the single channel idealization more accurate) mean that the idealized 1D ballistic theory sketched above is expected to apply. Indeed, recent measurements<sup>9</sup> of the period and amplitude of the zero-temperature persistent current in a  $\text{Ga}_{1-x}\text{Al}_x\text{As}/\text{GaAs}$  heterojunction found good agreement with detailed theoretical predictions<sup>6,11</sup> based on treating the electron motion as ballistic within a noninteracting electron-gas model.

The basic agreement between theory and experiment on persistent currents in semiconductor heterostructures means that one can begin to investigate more complex AB-like quantum interference effects in these systems. One of the

most natural extensions is an investigation of the influence of a *time-periodic* external magnetic field, leading to a time-periodic component of the flux. This line of investigation is also suggested by a number of prior studies of the influence of periodic external fields on mesoscopic systems, including investigations of electron transport through the time-modulated resonant tunneling devices<sup>12–16</sup> and harmonic generation in semiconductor superlattices.<sup>17</sup> Indeed, there have been previous theoretical studies of the effect of periodic external fields on various manifestations of the AB effect in mesoscopic systems.<sup>11,18–23</sup> We also would like to mention the papers<sup>24</sup> where the nonlinear response of the Aharonov-Bohm rings to time dependent fluxes has been studied in the context of Zener tunneling and localization in energy space.

In the present paper we study a 1D, single-channel, ballistic mesoscopic ring threaded by a constant magnetic flux and located in a resonant cavity to create an additional spatially inhomogeneous, time-periodic magnetic field (and hence flux). The electrons in the ring interact resonantly with the cavity ac magnetic field—described by a vector potential  $\mathbf{A}^{\text{RES}}(\varphi, t)$ —and with the constant Aharonov-Bohm vector potential ( $\mathbf{A}^{\text{AB}}$ ). The presence of  $\mathbf{A}^{\text{RES}}(\varphi, t)$  changes significantly the electron energy spectrum—turning it into a *quasienergy* spectrum, since the effective Hamiltonian is time periodic—and, *a priori*, can be expected to have strong effects on the AB oscillations in the observables of the mesoscopic system. We show that these effects can be interpreted within a suitable generalization of the “quantum nonlinear resonance” (QNR) theory first proposed by Berman and Zaslavsky<sup>25</sup> (see also Refs. 26–29). In particular, we find that when  $\mathbf{A}^{\text{RES}}(x, t)$  contains a single frequency, a single QNR occurs, whereas, when  $\mathbf{A}^{\text{RES}}(x, t)$  contains two frequencies, two QNR’s are formed, and their interactions can lead to “quantum chaos.” Thus time-dependent AB effects in mesoscopic rings can provide a novel experimental system, distinct from the widely studied problem of “Rydberg atoms” (Refs. 30–37)—i.e., the microwave ionization of hydrogen atoms prepared in highly excited (principal quantum number  $n_0 \gg 1$ ) states—in which to study the quantum nonlinear resonant phenomena and quantum chaos. In this regard, our results provide an explicit illustration of the utility of viewing mesoscopic systems with discrete spectra (quantum dots and small quantum rings) as “solid-state atoms.”<sup>17</sup> Note that, in recent experiments with mesoscopic systems influenced by the time-periodic fields, a quasienergy spectrum exhibits itself as well-known Rabi oscillations, Stark oscillations, harmonic generation (see, for example, Ref. 17), etc.

In the remainder of the paper, we present the details of our investigation. In Sec. II, we formulate the general problem, specify the details of the vector potentials, and derive a many-body Hamiltonian describing the dynamics of the electrons in the mesoscopic ring in the presence of the external fields. We then introduce a “resonant representation” which allows us to write an effective Hamiltonian that separates the slow (resonant) and fast dynamics and generalizes the original QNR approach<sup>25,26,28</sup> to the many-body case appropriate for our problem. In Sec. III, we prove that the case in which  $\mathbf{A}^{\text{RES}}(\varphi, t)$  contains a single frequency that corresponds to a single QNR, and we study the resulting resonant dynamics in

detail. We derive a general expression for the time-averaged shift of the ground-state energy  $\Delta E_0$  as a function of the amplitude of the AB flux, and the amplitude and frequency of the resonant external field. We evaluate  $\Delta E_0$  analytically in the weak-field limit, and then study the case for general field strength numerically. Our results show the presence of a sharp resonant enhancement, as a function of the cavity field frequency and/or AB flux, of the *amplitude* of the AB oscillations in the ground-state energy and hence in the persistent current. In Sec. IV, we examine explicitly the case when  $\mathbf{A}^{\text{RES}}(\varphi, t)$  contains two frequencies, establishing that two QNRs are formed and that their interaction (“overlap”) can lead to “quantum chaos” and a complex resonant structure for  $E_0(\Phi)$  and for the persistent current. We examine numerically the conditions for resonance overlap, and the transition to quantum chaos and discuss in detail the nature of the resonance structure in  $\Delta E_0$  in this regime. Finally, in Sec. V we summarize our results, comparing and contrasting them both with other studies of time-dependent AB effects in mesoscopic systems and with other systems (notably the Rydberg atoms) in which manifestations of quantum chaos have been observed. We provide estimates of the relevant ranges of parameters in which experimental verification of our results should be sought, and discuss open problems for further research. For purposes of completeness, in an Appendix we provide some essential background on the quantum nonlinear resonance approach and its relation to the more familiar classical nonlinear resonance theory.

## II. EFFECTIVE HAMILTONIAN FOR QUANTUM NONLINEAR RESONANCE

In this section we derive the effective Hamiltonian describing the dynamics of the noninteracting electrons in the external magnetic fields relevant to the physical situation we wish to study. Consider a small ballistic ring of the radius  $R$  placed in the  $(x, y)$  plane at the center of a cylindrical resonator of the radius  $r_0$ . Assume that the electrons in the ring are influenced by an external field which is described by the vector potential  $\mathbf{A}$  consisting of two parts,

$$\mathbf{A} = \mathbf{A}^{\text{AB}} + \mathbf{A}^{\text{RES}}(t), \quad (2.1)$$

where the Aharonov-Bohm potential is

$$\mathbf{A}^{\text{AB}} = (0, 0, A_\varphi^{\text{AB}}), \quad A_\varphi^{\text{AB}} = \frac{\Phi}{2\pi R}, \quad (2.2)$$

where  $\Phi$  is the corresponding magnetic flux. The vector potential  $\mathbf{A}^{\text{RES}}(t)$  in Eq. (2.1) describes the magnetic field created by the resonator’s eigenmodes. The solution for the  $n$ th eigenmode of the cylindrical resonator can be written in the form<sup>38</sup>

$$A_z^{\text{RES}} = 0, \quad (2.3)$$

$$A_r^{\text{RES}} = -n \left( \frac{H}{k^2 r} \right) \sin(n\varphi) J_n(kr) \cos(\omega t - k_z z),$$

$$A_\varphi^{\text{RES}} = -\frac{H}{k} \cos(n\varphi) J'_n(x) \Big|_{x=kr} \cos(\omega t - k_z z),$$

where  $J_n(x)$  is the Bessel function and  $J'(x) \equiv dJ(x)/dx$ . The frequency of this mode is

$$\omega^2 = c^2(k^2 + K_z^2). \quad (2.4)$$

The cavity boundary conditions imply that the wave vector  $k$  in Eq. (2.4) is quantized

$$k = \frac{K'_{nr}}{r_0} \quad (2.5)$$

where  $k'_{nr}$  is the  $r$ th zero of the function  $J'_n(x)$ . For example,

$$\begin{aligned} k'_{11} = 1.84, \quad k'_{12} = 5.33, \quad k'_{13} = 8.54, \\ k'_{01} = 3.83, \quad k'_{02} = 7.01. \end{aligned} \quad (2.6)$$

The wave vector  $k_z$  in Eq. (2.4) is determined by the boundary conditions along the  $z$  axis. If the resonator is infinite in the  $z$  direction, the value of  $k_z$  is arbitrary. In our geometry, the term  $k_z z$  in Eq. (2.3) merely adds a constant phase to the argument of  $\cos(\omega t - k_z z)$ , and, without loss of generality, we can choose it equal to zero. In Eq. (2.3), the constant  $H$  gives the order of magnitude of the magnetic field inside the resonator.

The most general case necessary for our later considerations involves a resonant potential having two frequencies, which means that we need to consider two eigenmodes in the resonator, having eigenfrequencies  $\omega_1$  and  $\omega_2$ . The other parameters of these eigenmodes will be specified shortly. In the absence of any vector potential, the electron's Hamiltonian is just the kinetic-energy term restricted to the ring, so that making the usual substitution  $\mathbf{p} \rightarrow (\mathbf{p} - e\mathbf{A}/c)$ , leads to a one-electron Hamiltonian of the form

$$\begin{aligned} \hat{H} = \frac{\hbar^2}{2mR^2} \left( \frac{\partial}{i\partial\varphi} - \alpha - \lambda_1 \sin(N\varphi) \cos\omega_1 t \right. \\ \left. - \lambda_2 \sin(M\varphi) \cos\omega_2 t \right)^2, \end{aligned} \quad (2.7)$$

where  $m$  is the effective electron mass and  $\varphi$  is the angle around the ring. Here  $\alpha$  is the dimensionless AB flux, and  $\lambda_{1,2}$  are the amplitudes of the resonant cavity modes:

$$\alpha = \frac{\Phi}{\Phi_0}, \quad \lambda_{1,2} = -\frac{2\pi R}{\Phi_0} \frac{H_{1,2}}{k_{1,2}} J'_{N,M}(k_{1,2}R). \quad (2.8)$$

The periodic boundary conditions appropriate for our ring geometry imply that the wave function of an electron is periodic in angle  $\varphi$  with the period  $2\pi$ :  $\Psi(\varphi + 2\pi, t) = \Psi(\varphi, t)$ . It is thus convenient to choose the functions

$$|n\rangle = \frac{1}{\sqrt{2\pi}} e^{in\varphi}, \quad n = 0, \pm 1, \pm 2, \dots \quad (2.9)$$

as a basis set. In essence, the resonance phenomena we analyze occur because of transitions induced by the cavity field among the electron levels of the ring. We are interested primarily in resonant processes near the Fermi level  $n_F$ , where the values of  $n$  are rather large:  $n \sim n_F \gg 1$ . In addition, we assume that the dimensionless amplitudes of the external

field are small on the scale of  $n_F$ :  $\lambda_{1,2} \ll n_F$ . We provide explicit estimates of the relevant physical parameters at the end of this section.

To first order in  $\lambda_{1,2}/n_F$ , from Eq. (2.7) we derive the one-electron dimensionless Hamiltonian  $\hat{H}_e$ ,

$$\begin{aligned} \hat{H}_e = \frac{2mR^2}{\hbar^2} \hat{H} \approx \left( \frac{\partial}{i\partial\varphi} - \alpha \right)^2 - 2 \left[ \lambda_1(t) \sin(N\varphi) \frac{\partial}{i\partial\varphi} \right. \\ \left. + \lambda_2(t) \sin(M\varphi) \frac{\partial}{i\partial\varphi} \right], \end{aligned} \quad (2.10)$$

where

$$\lambda_{1,2}(t) \equiv \lambda_{1,2} \cos\omega_{1,2}t. \quad (2.11)$$

In deriving Eq. (2.10), we have used the commutation relation

$$\left[ \frac{\partial}{i\partial\varphi}, \sin(n\varphi) \right] = -in \cos(n\varphi), \quad (2.12)$$

as well as the conditions  $N, M \ll n \sim n_F$ , reflecting our interest in considering resonances near the Fermi surface. Henceforth, we shall use  $\hat{H}_e$  of Eq. (2.10) to describe the electron dynamics in the external fields.

From Eq. (2.10) we have, for the matrix elements of the Hamiltonian  $\hat{H}_e$

$$\begin{aligned} \langle n | \hat{H}_e | n \rangle &= (n - \alpha)^2, \quad \langle n + N | \hat{H}_e | n \rangle = i\lambda_1(t)n, \\ \langle n - N | \hat{H}_e | n \rangle &= -i\lambda_1(t)n, \quad \langle n + M | \hat{H}_e | n \rangle = i\lambda_2(t)n, \\ \langle n - M | \hat{H}_e | n \rangle &= -i\lambda_2(t)n. \end{aligned} \quad (2.13)$$

These matrix elements define completely the one-electron Hamiltonian (2.10).

Since we are actually dealing with a many-electron problem, we must take into account the Pauli exclusion principle. Hence we introduce creation and annihilation operators  $\hat{c}_n^\dagger$  and  $\hat{c}_n$  for electrons in the  $n$ th energy level  $n$ , which satisfy the usual anticommutation relations  $\{\hat{c}_n, \hat{c}_{n'}^\dagger\}_+ = \delta_{n,n'}$ ,  $\{\hat{c}_n^\dagger, \hat{c}_{n'}^\dagger\}_+ = 0$ ,  $\{\hat{c}_n, \hat{c}_{n'}\}_+ = 0$ . In terms of these operators the Hamiltonian (2.10) takes the form

$$\begin{aligned} \hat{H}_e = \sum_n (n - \alpha)^2 \hat{c}_n^\dagger \hat{c}_n + i\lambda_1(t) \sum_n n \hat{c}_{n+N}^\dagger \hat{c}_n \\ - i\lambda_1(t) \sum_n n \hat{c}_{n-N}^\dagger \hat{c}_n + i\lambda_2(t) \sum_n n \hat{c}_{n+M}^\dagger \hat{c}_n \\ - i\lambda_2(t) \sum_n n \hat{c}_{n-M}^\dagger \hat{c}_n. \end{aligned} \quad (2.14)$$

In view of our focus on resonance effects in AB oscillations (an isolated quantum nonlinear resonance) and on the transition to quantum chaos, we have chosen to consider only the case of spinless electrons, since for these phenomena spin is an inessential complication.

We are interested in dynamical processes taking place in the vicinity of a level with quantum number  $n_* \gg 1$ . In this case, we can approximate the Hamiltonian  $\hat{H}_e$  by the expression

$$\begin{aligned}
\hat{H}_e \approx & \sum_n (n-\alpha)^2 \hat{c}_n^\dagger \hat{c}_n + i\Lambda_1(t) \sum_n \hat{c}_{n+N}^\dagger \hat{c}_n \\
& - i\Lambda_1(t) \sum_n \hat{c}_{n-N}^\dagger \hat{c}_n + i\Lambda_2(t) \sum_n \hat{c}_{n+M}^\dagger \hat{c}_n \\
& - i\Lambda_2(t) \sum_n \hat{c}_{n-M}^\dagger \hat{c}_n,
\end{aligned} \quad (2.15)$$

where

$$\Lambda_{1,2}(t) = \lambda_{1,2} n_* \cos \omega_{1,2} t. \quad (2.16)$$

A further simplification of the Hamiltonian (2.15) follows from measuring the levels with respect to  $n_*$ . Introducing the notations

$$n - n_* \equiv l, \quad (n - \alpha)^2 = (l - \alpha)^2 + n_*^2 + 2n_*(l - \alpha), \quad (2.17)$$

$$\hat{c}_n^\dagger = \hat{c}_{n_*+l}^\dagger \equiv \hat{c}_l^\dagger, \quad \hat{c}_n = \hat{c}_{n_{IL}+l} \equiv \hat{c}_l,$$

we can reexpress Eq. (2.15) as

$$\begin{aligned}
\hat{H}_e \approx & \sum_l [(l - \alpha)^2 + 2n_*(l - \alpha)] \hat{c}_l^\dagger \hat{c}_l \\
& + i\Lambda_1(t) \sum_l \hat{c}_{l+N}^\dagger \hat{c}_l - i\Lambda_1(t) \sum_l \hat{c}_{l-N}^\dagger \hat{c}_l \\
& + i\Lambda_2(t) \sum_l \hat{c}_{l+M}^\dagger \hat{c}_l - i\Lambda_2(t) \sum_l \hat{c}_{l-M}^\dagger \hat{c}_l.
\end{aligned} \quad (2.18)$$

In Eqs. (2.18) we dropped a term proportional to  $n_*^2$ , which merely adds a constant to the energy of the whole system.

Although it is not immediately evident, the Hamiltonian in Eqs. (2.18) includes both slowly oscillating terms describing the interesting “resonant” dynamics and the rapidly oscillating terms. Thus our next step is to separate explicitly the slow and fast dynamics by introducing a “resonant representation.”

We begin with the Schrödinger equation for an arbitrary Hamiltonian  $\hat{H}$ ,

$$i\hbar \frac{\partial |\Psi(t)\rangle}{\partial t} = \hat{H} |\Psi(t)\rangle, \quad (2.19)$$

and introduce a unitary operator  $\hat{U}(t)$  defining a wave function  $|\tilde{\Psi}(t)\rangle$  via

$$|\Psi(t)\rangle = \hat{U}(t) |\tilde{\Psi}(t)\rangle. \quad (2.20)$$

The wave function  $|\tilde{\Psi}(t)\rangle$  satisfies the Schrödinger equation

$$i\hbar \frac{\partial |\tilde{\Psi}(t)\rangle}{\partial t} = \hat{H}_{\text{eff}} |\tilde{\Psi}(t)\rangle, \quad (2.21)$$

with the effective Hamiltonian

$$\hat{H}_{\text{eff}} = \hat{U}^\dagger \hat{H} \hat{U} - i\hbar \hat{U}^\dagger \frac{\partial \hat{U}}{\partial t}. \quad (2.22)$$

To isolate the resonant, we write the operator  $\hat{U}(t)$  in the form

$$\hat{U} = \exp \left\{ -i\nu t \sum_n n \hat{c}_n^\dagger \hat{c}_n \right\}, \quad (2.23)$$

where the frequency  $\nu$  is at present an arbitrary parameter which we will later choose to remove the fast oscillations. Let

$$\tilde{\hat{c}}_{n'}(t) = \hat{U}^\dagger \hat{c}_{n'} \hat{U}. \quad (2.24)$$

Differentiating Eq. (2.24) and using the commutation relations, we derive the explicit time dependence of the operator  $\tilde{\hat{c}}_{n'}(t)$  as

$$\tilde{\hat{c}}_{n'}(t) = e^{-i\nu n' t} \hat{c}_{n'}. \quad (2.25)$$

Similarly, we have, for the operator  $\tilde{\hat{c}}_{n'}^\dagger(t)$ ,

$$\tilde{\hat{c}}_{n'}^\dagger(t) = \hat{U}^\dagger \hat{c}_{n'}^\dagger \hat{U} = e^{i\nu n' t} \hat{c}_{n'}^\dagger. \quad (2.26)$$

Finally, we need the operator equality

$$\hat{U}^\dagger \frac{\partial \hat{U}}{\partial t} = -i\nu \sum_n n \hat{c}_n^\dagger \hat{c}_n, \quad (2.27)$$

which follows directly from definition (2.23). Taking  $\hat{H} = (\hbar^2/2mR^2) \hat{H}_e$  and using Eqs. (2.23)–(2.26), we find that the Hamiltonian  $\hat{H}_{\text{eff}}$ , Eq. (2.22), can be written in the dimensionless form

$$\begin{aligned}
\hat{\mathcal{H}}_{\text{eff}} \equiv & \frac{2mR^2}{\hbar^2} \hat{H}_{\text{eff}} = \sum_l \left[ (l - \alpha)^2 + \left( 2n_* - \frac{2mR^2}{\hbar} \nu \right) l \right] \hat{c}_l^\dagger \hat{c}_l \\
& + i\Lambda_1(t) e^{i\nu N t} \sum_l \hat{c}_{l+N}^\dagger \hat{c}_l - i\Lambda_1(t) e^{-i\nu N t} \sum_l \hat{c}_{l-N}^\dagger \hat{c}_l \\
& + i\Lambda_2(t) e^{i\nu M t} \sum_l \hat{c}_{l+M}^\dagger \hat{c}_l - i\Lambda_2(t) e^{-i\nu M t} \sum_l \hat{c}_{l-M}^\dagger \hat{c}_l.
\end{aligned} \quad (2.28)$$

In deriving Eq. (2.28), we omitted the constant  $-2n_*(n_* + \alpha)$ , which does not depend on  $l$ , and thus only adds an additional phase to the wave function. This phase vanishes when calculating the expectation values. Below we shall use the Hamiltonian  $\hat{\mathcal{H}}_{\text{eff}}$ , Eq. (2.28), as the starting point for the calculation of the evolution of the wave function  $|\tilde{\Psi}(t)\rangle$  in Eq. (2.21).

To place the above formal manipulations in a more physical context, let us provide some estimates of the typical experimental values of the parameters in  $\hat{\mathcal{H}}_{\text{eff}}$ . From Ref. 9, we find that the typical electron (sheet) density is  $n \sim 4 \times 10^{11} \text{ cm}^{-2}$ , the electron mobility  $\mu \sim 10^6 \text{ cm}^2/\text{V s}$ , the Fermi velocity  $v_F \sim 3 \times 10^7 \text{ cm s}^{-1}$ , and the Fermi wavelength  $\lambda_F \sim 4 \times 10^{-6} \text{ cm}$ . The requirement that  $\lambda \ll n_F$ , which we used in deriving  $\hat{\mathcal{H}}_{\text{eff}}$ , can be expressed in the form

$$\lambda \approx \frac{\pi r_0 R H}{\Phi_0 k'_{nr}} \approx 8 \times 10^6 r_0 R H / k'_{nr} \ll n_F, \quad (2.29a)$$

where  $\Phi_0 \approx 4 \times 10^{-7}$  Oe cm<sup>2</sup> and all parameters are measured in cgs units. If  $k'_{nr} = k'_{11} \approx 1.84$ , condition (2.29a) takes the form

$$\lambda \approx 4.3 \times 10^6 r_0 R H \ll n_F, \quad (2.29b)$$

with  $H$  expressed in Oe and  $R$  and  $r_0$  expressed in cm. This translates into an upper limit on the strength of the resonant field in Oe,

$$H < H_{cr} = \frac{n_F k'_{nr}}{8 \times 10^6 r_0 R} \text{ Oe}, \quad (2.29c)$$

which for typical parameter values ( $R = 10^{-4}$  cm,  $r_0 = 0.1$  cm, and  $n_F = 10^2 - 10^3$ , and  $k'_{nr} \sim 2$  is  $H_{cr} = 2.5 - 25$  Oe.

The condition  $L = 2\pi R < l_{el}$ , where  $l_{el}$  is the elastic mean free path, is easily satisfied by micrometer-sized rings, since at low temperature  $l_{el}$  can be of the order of several tens of micrometers for high-electron-mobility Ga<sub>1-x</sub>Al<sub>x</sub>As/GaAs heterojunction structures.<sup>9,17,39,40</sup>

### III. AN ISOLATED QUANTUM NONLINEAR RESONANCE

#### A. Effective Hamiltonian for an isolated QNR

An isolated QNR occurs when the resonant external field has only a single eigenmode with frequency  $\omega_1 \equiv \omega$ . Thus in our general expression (2.28) for the resonant Hamiltonian we should set

$$\Lambda_1(t) \equiv \Lambda(t), \quad \Lambda_2(t) = 0. \quad (3.1)$$

Introducing a dimensionless time variable via

$$\tau = \kappa t \quad \left( \kappa = \frac{\hbar}{2mR^2} \right), \quad (3.2)$$

we can write the Schrödinger equation for the wave function  $|\tilde{\Psi}(\tau)\rangle$  as

$$i \frac{\partial |\tilde{\Psi}(\tau)\rangle}{\partial \tau} = \hat{\mathcal{H}}_{\text{eff}} |\tilde{\Psi}(\tau)\rangle, \quad (3.3)$$

where for  $\hat{\mathcal{H}}_{\text{eff}}$  we have, from Eq. (2.28), using Eqs. (3.1) and (3.2),

$$\begin{aligned} \hat{\mathcal{H}}_{\text{eff}} = & \sum_l [(l - \alpha)^2 + (2n_* - \nu/\kappa)] \hat{c}_l^\dagger \hat{c}_l \\ & + i\Lambda(\tau) e^{i\nu N\tau/\kappa} \sum_l \hat{c}_{l+N}^\dagger \hat{c}_l \\ & - i\Lambda(\tau) e^{-i\nu N\tau/\kappa} \sum_l \hat{c}_{l-N}^\dagger \hat{c}_l. \end{aligned} \quad (3.4)$$

Consider the time-dependent term in Eq. (3.4). From definitions (2.11) and (2.16), we find

$$\Lambda(\tau) e^{\pm i\nu N\tau/\kappa} = \frac{\Lambda}{2} (e^{i\omega\tau/\kappa} + e^{-i\omega\tau/\kappa}) e^{\pm i\nu N\tau/\kappa}$$

with

$$\Lambda \equiv \lambda_1 n_*. \quad (3.5)$$

Choosing

$$\nu = \omega/N \quad (3.6)$$

removes the time dependence from half the terms in Eq. (3.5), and causes the remainder to oscillate at high frequency. Neglecting these high frequency terms—the so-called “rotating wave approximation” (RWA), which is standard in discussions of QNR (Ref. 25)—implies that

$$\Lambda(\tau) e^{\pm i\nu N\tau/\kappa} \approx \frac{\Lambda}{2}. \quad (3.7)$$

Hence within the RWA the Hamiltonian  $\hat{\mathcal{H}}_{\text{eff}}$ , Eq. (3.4), is time independent and assumes the form

$$\hat{\mathcal{H}}_{\text{eff}} = \sum_l E_l \hat{c}_l^\dagger \hat{c}_l + i \frac{\Lambda}{2} \sum_l \hat{c}_{l+N}^\dagger \hat{c}_l - i \frac{\Lambda}{2} \sum_l \hat{c}_{l-N}^\dagger \hat{c}_l, \quad (3.8)$$

where

$$E_l = (l - \alpha)^2 + (2n_* - \omega/N\kappa)l, \quad (l = n - n_*). \quad (3.9)$$

If we now assume that the frequency  $\omega$  of the external field is resonant with the transitions between the levels with numbers  $n$  and  $N+n$  of the system in the absence of the time-dependent field, then the resonant condition can be written in the form

$$\left. \frac{E_{N+n}^{(0)} - E_n^{(0)}}{\hbar} \right|_{n=n_r} = \kappa [N^2 + 2N(n - \alpha)]|_{n=n_r} = \omega, \quad (3.10)$$

where  $E_n^{(0)}$  is the eigenvalue of the unperturbed Hamiltonian  $\hat{H}_0$

$$\hat{H}_0 = \frac{\hbar^2}{2mR^2} \left( \frac{\partial}{i\partial\varphi} - \alpha \right)^2, \quad E_n^{(0)} = \frac{\hbar^2}{2mR^2} (n - \alpha)^2. \quad (3.11)$$

The solution of Eq. (3.10) defines the resonant level  $n = n_r$  (the center of an isolated QNR) as

$$n_r = [\alpha + \omega/2N\kappa - N/2]_{\text{int}}, \quad (3.12)$$

where  $[x]_{\text{int}}$  is the integer part of  $x$ . Note that Eq. (3.10) for  $n_*$  coincides with the equation

$$(E_{N+l} - E_l)|_{l=0} = 0, \quad (3.13)$$

where  $E_l$  is defined in Eq. (3.9).

The resonance couples only levels differing by  $N$  units, and thus the expression for the Hamiltonian (3.8) can be significantly simplified by introducing  $N$  subsequences of levels. Formally, we replace the index  $n$  by  $k + lN$  according to the rule

$$\begin{aligned} \hat{c}_n \rightarrow \hat{c}_{k+lN} & \equiv \hat{b}_l(k), \quad k = n_0, \dots, n_0 + N - 1, \\ l & = 0, \pm 1, \pm 2, \dots, \end{aligned} \quad (3.14)$$

where  $n_0$  is an arbitrary number. (Below, we shall assume that  $n_0 \sim n_* \sim n_F \gg 1$ .) With this substitution, we can reexpress the Hamiltonian in a form that makes explicit its de-

composition into  $N$  independent terms that reflect the couplings among the separate towers of states. We find

$$\hat{\mathcal{H}}_{\text{eff}} = \sum_{k=n_0}^{n_0+N-1} \hat{\mathcal{H}}_{\text{eff}}(k), \quad (3.15)$$

where

$$\begin{aligned} \hat{\mathcal{H}}_{\text{eff}}(k) = & \sum_l \varepsilon_{l,k} \hat{b}_l^\dagger(k) \hat{b}_l(k) + i \frac{\Lambda}{2} \sum_l \hat{b}_{l+1}^\dagger(k) \hat{b}_l(k) \\ & - i \frac{\Lambda}{2} \sum_l \hat{b}_{l-1}^\dagger(k) \hat{b}_l(k) \end{aligned} \quad (3.16)$$

and

$$\varepsilon_{l,k} = (k + lN - n_* - \alpha)^2 + (2n_* - \omega/N\kappa)(k + lN - n_*). \quad (3.17)$$

The Hamiltonian (3.15) can be used for calculation of all observables in our system.

### B. Expression for the expectation value of the energy shift

The expression for the time-dependent expectation value of the energy of the system is

$$\begin{aligned} E(\tau) &= \langle \Psi(\tau) | \sum_n (n - \alpha)^2 \hat{c}_n^\dagger \hat{c}_n | \Psi(\tau) \rangle \\ &= \langle \tilde{\Psi}(\tau) | \hat{U}^\dagger \sum_n (n - \alpha)^2 \hat{c}_n^\dagger \hat{c}_n \hat{U} | \tilde{\Psi}(\tau) \rangle \\ &= \langle \tilde{\Psi}(\tau) | \sum_n (n - \alpha)^2 \hat{c}_n^\dagger \hat{c}_n | \tilde{\Psi}(\tau) \rangle. \end{aligned} \quad (3.18)$$

We shall evaluate this expression in the Heisenberg representation. Then, according to Eq. (2.21), the operator equation for an arbitrary operator  $\hat{f}$  has the form

$$\frac{\partial \hat{f}}{\partial \tau} = i[\hat{\mathcal{H}}_{\text{eff}}, \hat{f}], \quad (3.19)$$

where the Hamiltonian  $\hat{\mathcal{H}}_{\text{eff}}$  is defined in Eq. (3.15). Using  $[c_m^\dagger \hat{c}_n, \hat{c}_k] = -\delta_{k,m} \hat{c}_n$  and the definitions (3.14), we can derive immediately the Heisenberg equations of motion for the operators  $\hat{b}_l(k)$ :

$$\frac{\partial \hat{b}_l(k)}{\partial \tau} = -i\varepsilon_{l,k} \hat{b}_l(k) + \frac{\Lambda}{2} \hat{b}_{l-1}(k) - \frac{\Lambda}{2} \hat{b}_{l+1}(k). \quad (3.20)$$

We seek a solution to this equation in the form of an expansion in the operators at the initial time  $\tau=0$ ,

$$\hat{b}_l(\tau, \kappa) = \sum_{l'} i^l a_{l,l'}(\tau) \hat{b}_{l'}(k), \quad (3.21)$$

where the  $a_{l,l'}(\tau)$  are time-dependent  $c$ -number coefficients. Substituting Eq. (3.21) into Eq. (3.20), we find a system of equations for the coefficients  $a_{l,l'}(\tau)$ :

$$i\dot{a}_{l,l'} = \varepsilon_{l,k} a_{l,l'} + \frac{\Lambda}{2} a_{l-1,l'} + \frac{\Lambda}{2} a_{l+1,l'}. \quad (3.22)$$

These equations must be solved with the initial conditions

$$a_{l,l'}(\tau=0) = i^{-l'} \delta_{l,l'}. \quad (3.23)$$

To relate the system of equations (3.22) to the canonical form of the “quantum nonlinear resonance” equations,<sup>25,28</sup> we introduce the function

$$\Phi(\theta, \varphi, \tau) \equiv \sum_{l,l'} a_{l,l'}(\tau) e^{i(l\theta + l'\varphi)} = \Phi(\theta + 2\pi, \varphi + 2\pi, \tau), \quad (3.24)$$

where the coefficients  $a_{l,l'}(\tau)$  satisfy Eqs. (3.22).  $\Phi$  is actually the wave function, in the action-angle representation, describing the slow dynamics in the vicinity of the QNR. Specifically, from Eq. (3.22), we find that  $\Phi(\theta, \varphi, \tau)$  satisfies the Schrödinger equation

$$i \frac{\partial \Phi}{\partial \tau} = \hat{H}_r^{(k)} \left( \theta, -i \frac{\partial}{\partial \theta} \right) \Phi, \quad (3.25a)$$

where the Hamiltonian  $\hat{H}_r^{(k)}$  is of the form

$$\hat{H}_r^{(k)} \left( \theta, -i \frac{\partial}{\partial \theta} \right) \equiv \hat{\varepsilon} \left( -i \frac{\partial}{\partial \theta}, k \right) + \Lambda \cos \theta. \quad (3.25b)$$

According to Eq. (3.17), the unperturbed part of the Hamiltonian (3.25b) is given by the expression

$$\begin{aligned} \hat{\varepsilon} \left( -i \frac{\partial}{\partial \theta}, k \right) &\equiv \left( k - iN \frac{\partial}{\partial \theta} - n_* - \alpha \right)^2 + \left( 2n_* - \frac{\omega}{N\kappa} \right) \\ &\times \left( k - iN \frac{\partial}{\partial \theta} - n_* \right). \end{aligned} \quad (3.26)$$

The Schrödinger equation (3.25a) with the Hamiltonian (3.25b) has the canonical form of the equation for an isolated QNR (see, e.g., Refs. 25–28), and describes a slow resonant dynamics of the system in a vector potential of the form (2.1) with one resonant frequency of the external ac field. In the Appendix, we also show how this equation provides insight into the corresponding “classical limit” and the classical theory of nonlinear resonances.

For our present purposes, it is most useful to solve Eq. (3.22) directly. Substituting

$$a_{l,l'}(\tau) = e^{-i\varepsilon\tau} A_{l,l'}, \quad (3.27)$$

into Eq. (3.22) leads to a set of eigenvalue equations for the quasienergy eigenfunctions

$$\varepsilon A_{l,l'} = \varepsilon_{l,k} A_{l,l'} + \frac{\Lambda}{2} (A_{l-1,l'} + A_{l+1,l'}). \quad (3.28)$$

We denote the eigenvalues of Eq. (3.28) by  $\varepsilon_\sigma$ , and the corresponding eigenfunctions by  $A_l^{(\sigma)}$ , with the index  $\sigma$  labeling the distinct eigenfunctions, and  $l = n - n_*$  defining the  $l$ th component of the eigenfunction in the unperturbed basis (2.9). The matrix  $A_{l,l'}$  in Eq. (3.28) is symmetric and has real coefficients, so that the eigenfunctions  $A_l^{(\sigma)}$  can be chosen real. The general solution of Eq. (3.22) can then be written as

$$a_{l,l'}(\tau) = \sum_\sigma e^{-i\varepsilon_\sigma \tau} S_\sigma^{(l'l')} A_l^{(\sigma)}, \quad (3.29)$$

where the expansion coefficients  $S_{\sigma}^{(l')}$  satisfy the equation

$$i^{l'} \sum_{\sigma} S_{\sigma}^{(l')} A_l^{(\sigma)} = \delta_{l,l'}. \quad (3.30)$$

Using the orthogonality properties of the eigenfunctions  $A^{(\sigma)}$ ,

$$\sum_l A_l^{(\sigma)} A_l^{(\sigma')} = \delta_{\sigma,\sigma'}, \quad \sum_{\sigma} A_l^{(\sigma)} A_{l'}^{(\sigma)} = \delta_{l,l'}, \quad (3.31)$$

we find that the expansion coefficients  $S_{\sigma}^{(l)}$  can be written as

$$S_{\sigma}^{(l)} = (-i)^l A_l^{(\sigma)}. \quad (3.32)$$

Substituting Eq. (3.32) into Eqs. (3.21) and (3.28), we obtain

$$a_{l,l'}(\tau) = (-i)^{l'} \sum_{\sigma} e^{-i\epsilon_{\sigma}\tau} A_{l'}^{(\sigma)} A_l^{(\sigma)}, \quad (3.33)$$

$$\hat{b}_l(\tau, k) = i^l \sum_{l'} \sum_{\sigma} (-i)^{l'} e^{-\epsilon_{\sigma}\tau} A_{l'}^{(\sigma)} A_l^{(\sigma)} \hat{b}_{l'}(k). \quad (3.34)$$

Combining the various transformations, we find that in terms of the operators  $\hat{b}_l^{\dagger}(\tau, k)$ ,  $\hat{b}_l(\tau, k)$  Eq. (3.18) for the time-dependent average energy takes the form

$$E(\tau) = \langle \Psi_0 | \sum_k \sum_l (k + lN - \alpha)^2 \hat{b}_l^{\dagger}(\tau, k) \hat{b}_l(\tau, k) | \Psi_0 \rangle. \quad (3.35)$$

Here,  $|\Psi_0\rangle$  is the ground state of the unperturbed system, with all levels up to  $n_F$  occupied by electrons.

It is easily seen that only the diagonal part of  $\hat{b}_l^{\dagger}(\tau, k) \hat{b}_l(\tau, k)$  contributes to  $E(\tau)$ , namely,

$$\begin{aligned} \hat{b}_l^{\dagger}(\tau, k) \hat{b}_l(\tau, k) &\rightarrow \sum_{\sigma, \sigma'} e^{i(\epsilon_{\sigma} - \epsilon_{\sigma'})\tau} A_l^{(\sigma)} A_l^{(\sigma')} \\ &\times \sum_{l'} A_{l'}^{(\sigma)} A_{l'}^{(\sigma')} \hat{b}_{l'}^{\dagger}(k) \hat{b}_{l'}(k). \end{aligned} \quad (3.36)$$

Using Eq. (3.36), from Eq. (3.35) we derive

$$\begin{aligned} E(\tau) &= \sum_{k,l} (k + lN - \alpha)^2 \sum_{\sigma, \sigma'} e^{i(\epsilon_{\sigma} - \epsilon_{\sigma'})\tau} A_l^{(\sigma)} A_l^{(\sigma')} \\ &\times \sum_{l'} A_{l'}^{(\sigma)} A_{l'}^{(\sigma')} \langle \Psi_0 | \hat{b}_{l'}^{\dagger}(k) \hat{b}_{l'}(k) | \Psi_0 \rangle. \end{aligned} \quad (3.37)$$

In the absence of the ac external field ( $\Lambda = 0$ ), the expectation value of the energy is

$$E_0 = \sum_{k,l} (k + lN - \alpha)^2 \langle \Psi_0 | \hat{b}_l^{\dagger}(k) \hat{b}_l(k) | \Psi_0 \rangle, \quad (3.38)$$

and of course coincides with the ground-state energy.

From the translation invariance of the sums when  $\alpha$  is shifted by an integer, one can see that  $E(\tau)$  and  $E_0$  are periodic functions of the magnetic flux  $\alpha$ , with the period 1 (the fundamental period  $\Phi_0$ ). Hence we can consider these functions only in the region  $0 \leq \alpha \leq 1$ . The expression for  $E(\tau)$

can be simplified by expanding the unperturbed spectrum in the vicinity of the large number  $n_*$ ,

$$\begin{aligned} (n - \alpha)^2 &= (n_* + n - n_* - \alpha)^2 \\ &= n_*^2 + (n - n_* - \alpha)^2 + 2n_*(n - n_* - \alpha). \end{aligned} \quad (3.39)$$

The  $n_*^2$  term in Eq. (3.39) does not influence the  $\alpha$  dependence of the energy shift, and can be ignored for our considerations. Further, we can neglect the term proportional to  $(n - n_* - \alpha)^2$ , as it gives a small contribution to the average energy shift in the relevant limit  $n_* \gg |n - n_* - \alpha|$ . With these approximations, elementary algebra leads from Eq. (3.37) to the final expression for the expectation value of the energy shift induced by the ac external field:

$$\begin{aligned} \Delta E_0(\tau) &\equiv \frac{1}{2Nn_*} [E(\tau) - E_0] \\ &= \sum_{k,l} l \left\{ \sum_{\sigma, \sigma'} e^{i(\epsilon_{\sigma} - \epsilon_{\sigma'})\tau} A_l^{(\sigma)} A_l^{(\sigma')} \sum_{l'} A_{l'}^{(\sigma)} A_{l'}^{(\sigma')} \right. \\ &\quad \times \langle \Psi_0 | \hat{b}_{l'}^{\dagger}(k) \hat{b}_{l'}(k) | \Psi_0 \rangle \\ &\quad \left. - \langle \Psi_0 | \hat{b}_l^{\dagger}(k) \hat{b}_l(k) | \Psi_0 \rangle \right\}. \end{aligned} \quad (3.40)$$

In deriving this equation we have neglected terms independent of  $l$  (which are proportional to the constants  $k$ ,  $n_*$ , and  $\alpha$ ), as these terms do not contribute to  $\Delta E_0(\tau)$ . Note that the dependence on the flux  $\alpha$  in Eq. (3.40) is contained in the eigenfunctions  $A_l^{(\sigma)}$  and in the eigenvalues  $\epsilon_{\sigma}$ . The function  $\langle \Psi_0 | \hat{b}_l^{\dagger}(k) \hat{b}_l(k) | \Psi_0 \rangle$  in Eq. (3.40) has the simple form

$$\langle \Psi_0 | \hat{b}_l^{\dagger}(k) \hat{b}_l(k) | \Psi_0 \rangle = \begin{cases} 1 & \text{if } k + lN \leq n_F \\ 0 & \text{if } k + lN > n_F. \end{cases} \quad (3.41)$$

To exhibit the resonance structure most simply, we can study the time average of the expectation value of the ground-state energy shift,

$$\begin{aligned} \Delta E_0 &\equiv \lim_{T \rightarrow \infty} \frac{1}{T} \int_0^T \Delta E_0(\tau) d\tau \\ &= \sum_{k,l} l \left\{ \sum_{\sigma} (A_l^{(\sigma)})^2 \sum_{l'} (A_{l'}^{(\sigma)})^2 \langle \Psi_0 | \hat{b}_{l'}^{\dagger}(k) \hat{b}_{l'}(k) | \Psi_0 \rangle \right. \\ &\quad \left. - \langle \Psi_0 | \hat{b}_l^{\dagger}(k) \hat{b}_l(k) | \Psi_0 \rangle \right\}. \end{aligned} \quad (3.42)$$

In Secs. III C and III D, we study the dependence of  $\Delta E_0$  on the AB flux ( $\alpha$ ) and on the amplitude ( $\Lambda$ ) and frequency  $\omega$  of the ac external field, first analytically in the weak-field limit, and then numerically in general. For definiteness in our calculations, we shall assume that the number of spinless electrons in the ring is odd,  $n_e = 2N_e + 1$ . (We shall discuss the case of even  $n_e$  briefly later.) For odd  $n_e$ , at  $\alpha = 0$ , the population of electrons in the ground state is symmetric, for positive and negative momenta,  $l$ . The relation between the Fermi level  $n_F$  and the Fermi frequency  $\omega_F$  is

$$|n_F(\alpha=0)| = N_e = \frac{\omega_F}{2N\kappa}, \quad (3.43)$$

where, as in Eq. (3.2),  $\kappa = \hbar/(2mR^2)$ . Let us also introduce the dimensionless detuning in frequency from  $\omega_F$  via

$$\omega_0 = \frac{1}{2N\kappa} (\omega - \omega_F). \quad (3.44)$$

There is a simple symmetry which enables one to reduce the summation over momenta,  $l$ , in Eq. (3.42) to positive values only: namely,

$$\Delta E_0^{(-)}(\alpha) = \Delta E_0^{(+)}(1 - \alpha), \quad \alpha \neq 0.5,$$

where we have introduced the notation  $\Delta E^{(+)}(\Delta E^{(-)})$  to indicate the sum over positive (negative) values of  $l$  only. Using this relation the expression for  $\Delta E_0(\alpha)$  in Eq. (3.42) can be written in the form

$$\Delta E_0(\alpha) = \Delta E_0^{(+)}(\alpha) + \Delta E_0^{(+)}(1 - \alpha), \quad \alpha \neq 0.5. \quad (3.45)$$

This result was used to simplify the numerical calculations. For the case  $\alpha = 0.5$ , for reasons discussed below, the contributions to  $\Delta E_0(\alpha)$  from positive and negative  $l$  were calculated separately. Before presenting our detailed numerical results on  $\Delta E_0$  in the general case, we provide some analytic insight into the behavior in the weak-field limit.

### C. Analytic results in the weak-field limit

The resonant dependence of the function  $\Delta E_0$  on  $\alpha$  for small  $\Lambda$  can be studied analytically using a ‘‘two-level approximation,’’ because, for any  $N$ , when  $\Lambda \ll 1$ , only the two levels nearest  $n_F$  (corresponding to  $l=0$  and  $l=1$ ) give leading contributions to  $\Delta E_0$ . In this case, Eq. (3.28) become

$$\epsilon A_1 = \epsilon_1 A_1 + \frac{\Lambda}{2} A_0, \quad (3.46)$$

$$\epsilon A_0 = \epsilon_0 A_0 + \frac{\Lambda}{2} A_1,$$

where  $\mathbf{A} = (A_0, A_1)$  is the quasienergy eigenfunction [in this case  $\sigma = 1, 2$  in Eq. (3.29)]. The corresponding quasienergies are given by the explicit expressions

$$\epsilon_{1,2} = \frac{\epsilon_1 + \epsilon_0}{2} \pm \frac{1}{2} \sqrt{(\epsilon_1 - \epsilon_0)^2 + \Lambda^2/4}. \quad (3.47)$$

In Eq. (3.47) the unperturbed energy levels  $\epsilon_1$  and  $\epsilon_0$  are defined by Eq. (3.17). To calculate the expression  $\Delta E_0$  from Eq. (3.42), we need the following components of the quasienergy eigenfunctions:

$$A_1^{(1)} = \frac{\Lambda/2}{\sqrt{(\epsilon_1 - \epsilon_1)^2 + (\Lambda/2)^2}}, \quad (3.48)$$

$$A_1^{(2)} = \frac{\Lambda/2}{\sqrt{(\epsilon_1 - \epsilon_2)^2 + (\Lambda/2)^2}}.$$

Using Eqs. (3.48), we obtain from Eq. (3.42) the expression for  $\Delta E_0$ ,

$$\Delta E_0 = 1 - \frac{(\Lambda/2)^4}{\left\{ \left[ \frac{(\epsilon_1 - \epsilon_0)}{2} - \sqrt{\left( \frac{\epsilon_1 - \epsilon_0}{2} \right)^2 + \left( \frac{\Lambda}{2} \right)^2} \right]^2 + \left( \frac{\Lambda}{2} \right)^2 \right\}} - \frac{(\Lambda/2)^2}{\left\{ \left[ \frac{(\epsilon_1 - \epsilon_0)}{2} + \sqrt{\left( \frac{\epsilon_1 - \epsilon_0}{2} \right)^2 + \left( \frac{\Lambda}{2} \right)^2} \right]^2 + \left( \frac{\Lambda}{2} \right)^2 \right\}}. \quad (3.49)$$

In deriving this equation, we used

$$\langle \Psi_0 | \hat{b}_l^\dagger \hat{b}_l | \Psi_0 \rangle = \begin{cases} 1 & \text{if } l=0 \\ 0 & \text{if } l=1. \end{cases} \quad (3.50)$$

The width of the resonance  $\delta\alpha$  in this approximation satisfies  $\delta\alpha \sim \Lambda$ . In Sec. III D we shall compare these analytic predictions with our full numerical simulations in the limit  $\Lambda \ll 1$ .

Our two-level calculation illustrates an important feature of this resonance phenomenon, which will later emerge from our numerics and may be significant for experimental observations: namely, one can observe the resonance *either* by fixing the AB flux  $\alpha$  and tuning the frequency  $\omega$ , or by fixing the frequency  $\omega$  and sweeping through values of  $\alpha$ . To see this in the present case, note that the energy shift  $\Delta E_0$  in Eq. (3.49) depends on the value  $\epsilon_1 - \epsilon_0$ . From Eq. (3.17) and definitions (3.2), (3.43), and (3.44), we have

$$\epsilon_1 - \epsilon_0 = 1 - 2\alpha - 2\omega_0, \quad (3.51)$$

where we have chosen  $N=1$ ,  $k=n_0=n_*=n_F$ . From Eq. (3.49), we see that the center of the resonance is located at  $\epsilon_1 - \epsilon_0 = 0$ , which, according to Eq. (3.51), is equivalent to the condition  $\alpha + \omega_0 = 0.5$ . If  $\omega_0 = 0$ , the center of the resonance occurs at  $\alpha = 0.5$ . At  $\alpha = 0$ , the center of the resonance depends on the frequency of detuning, and occurs at  $\omega_0 = 0.5$ . Hence sweeping through either variable with the other fixed will yield the resonance structure.

### D. Numerical studies of an isolated QNR

We preface the discussion of our numerical simulations with several clarifying comments. For  $n_e \gg 1$ , the resonant transitions take place in the vicinity of the Fermi surface, and can be considered separately for positive and negative momenta  $l$ . In this case, it is convenient to introduce the Fermi levels  $n_F^{(\pm)}$ , corresponding to positive and negative  $l$ . Let us write the flux  $\alpha$  as a sum of two parts, an integer part  $n_\alpha$  and a fractional part,  $\xi_\alpha$

$$\alpha = n_\alpha + \xi_\alpha, \quad (3.52)$$

where  $n_\alpha = [\alpha]_{\text{int}}$ ,  $\xi_\alpha = \{\alpha\}_{\text{frac}}$ , ( $0 \leq \xi_\alpha < 1$ ). Then, the position of Fermi level for  $l > 0$  can be written in the form

$$n_F^{(+)} = \begin{cases} n_\alpha + N_e & \text{if } \xi_\alpha \leq 0.5 \\ n_\alpha + N_e + 1 & \text{if } \xi_\alpha > 0.5. \end{cases} \quad (3.53)$$



To exclude large numbers  $n \sim n_F \sim 10^2 - 10^4$  in the numerical experiment, it is convenient to use the system of reference—namely, the resonant level  $n = n_r$ —introduced in Eq. (3.12). This level defines the center of an isolated QNR, where the dominant dynamical effects occur. We express the level  $n_r$  in Eq. (3.12) in the form

$$n_r = \left[ \alpha + \frac{\omega}{N\kappa} - \frac{N}{2} \right]_{\text{int}} = N_e + n_\alpha + \left[ \xi_\alpha + \omega_0 - \frac{N}{2} \right]_{\text{int}}. \quad (3.54)$$

We can now specify the levels  $n_*$  and  $n_0$  which were introduced above in Eqs. (2.17) and (3.14). Specifically, we set

$$n_* = n_0 = n_r, \quad (3.55)$$

and for convenience introduce the variables

$$\bar{k} = k - n_r, \quad \bar{n}_F^{(+)} = n_F^{(+)} - n_r \quad (\bar{k} \in [0, N-1]). \quad (3.56)$$

Then, from Eq. (3.53) we find

$$\bar{n}_F^{(+)} = \begin{cases} -[\xi_\alpha + \omega_0 - N/2]_{\text{int}} & \text{if } \xi_\alpha \leq 0.5 \\ 1 - [\xi_\alpha + \omega_0 - N/2]_{\text{int}} & \text{if } \xi_\alpha > 0.5. \end{cases} \quad (3.57)$$

In this notation the spectrum  $\epsilon_{l,k}$ , Eq. (3.17), is

$$\epsilon_{l,\bar{k}} = (\bar{k} + lN)^2 + 2(\bar{k} + lN)([\xi_\alpha + \omega_0 - N/2]_{\text{int}} - \omega_0 + \xi_\alpha). \quad (3.58)$$

If, for example, we put  $\omega_0 = 0$ ,  $N = 1$ , spectrum (3.58) takes the simple form

$$\epsilon_{l,\bar{k}} = (l - \xi_\alpha)^2. \quad (3.59)$$

This equation illustrates a very important subtlety that must be properly finessed in the numerics: namely, at certain points there can be *degeneracies* in the spectrum which can cause problems in evaluating quantities such as time averages. Examining Eq. (3.59) shows that at the points  $\xi_\alpha = 0$  and  $\xi_\alpha = 0.5$  the unperturbed spectrum of the Hamiltonian in Eq. (3.25) becomes degenerate [this degeneracy also occurs in the general case (3.58) for some values of  $\xi_\alpha$ ]. This degeneracy results in very small differences of quasienergies  $\Delta\epsilon_i$  for some quasienergy eigenfunctions, and time-average energy (3.42) becomes ill defined at these values of  $\xi_\alpha$ . Specifically, the quasidegenerate symmetric and antisymmetric eigenfunctions give a contribution to  $\Delta E_0(\alpha)$ , Eq. (3.42), in this case. Some of these functions describe nearly free-electron dynamics and hence describe large energy motions ( $\sim n_F$ ). Actually, this phenomenon leads to exponentially large times of electron tunneling in the region of large energies and is not observable in the types of systems we consider here. To exclude these “dangerous” points  $\xi_\alpha = 0$  and  $0.5$ , we should include some additional terms (which would arise from some small additional interactions that split the degeneracy) in the unperturbed spectrum (3.59) and in Eq. (3.58), so that the symmetry of the eigenvalue problem for system (3.25) is broken and the quasidegeneracy destroyed. In real physical systems, these small terms always exist and can be connected, for example, with crystal-field effects. Indeed, it is easy to show that these additional terms are of the

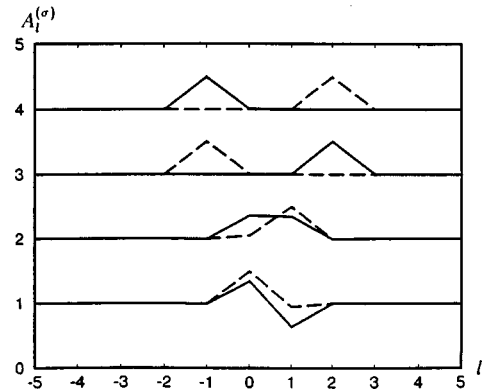


FIG. 1. Dependence of the quasienergy functions  $A_l^{(\sigma)}$  on  $l$ :  $\sigma = 1, 2, 3, 4$ ;  $\Lambda = 0.001$ ;  $\omega_0 = 0$ ; and  $\alpha = 0.5$  (solid curve); and  $\alpha = 0.495$  (dashed curve).

order  $\delta n \sim (n - n_* - \alpha)^3 / n_*$ , and in our case ( $n_* \sim n_F \sim 10^2 - 10^4$ ) can be estimated to be of order  $\delta n \sim 10^{-4} - 10^{-2}$ .

To remove these quasidegeneracies in our numerics we can either add the small symmetry-breaking term  $\delta n \sim (n - n_* - \alpha)^3 / n_*$ , or we can add a random number of order  $\delta n \sim 10^{-2} - 10^{-4}$  to the unperturbed spectrum. The results of our numerical calculations do not depend on the procedure we use to avoid this quasidegeneracy.

We begin the discussion of our numerical results with the case of a resonant field with  $\omega = \omega_F$  ( $\omega_0 = 0$ ) and small amplitude. In this case, the dynamics should be described by the two-level approximation examined analytically in Sec. III C. Figure 1 provides numerical evidence justifying this approximation: for  $\Lambda = 10^{-3}$ , Fig. 1 demonstrates that only two quasienergy levels (with  $\sigma = 1, 2$ ) are involved in the electron dynamics, and respond significantly to small variation of the AB flux  $\alpha$  in the vicinity of  $\alpha = 0.5$ . Moreover, for small deviations of the AB flux (e.g.,  $\alpha = 0.495$ ) the quasienergy eigenfunctions with  $\sigma = 1, 2$  already include only one level of the unperturbed Hamiltonian. This means that no real dynamics happens in the system in this latter case. At the same time, when  $\alpha = 0.5$ , and the resonant condition is satisfied, two levels of the unperturbed Hamiltonian contribute to the eigenfunctions with  $\sigma = 1, 2$ , and this results in a very narrow resonance in  $\Delta E_0(\mu = 0.5)$ ; this is shown in Fig. 2. The quasienergy levels with  $\sigma = 3, 4$  include only one level of the unperturbed Hamiltonian, and actually do not change their behavior (but only interchange roles) when the magnetic flux is varied in the vicinity of the resonance at  $\alpha = 0.5$ . From the blowup in Fig. 2(b), we see that the resonance is quite sharp in  $\alpha$ , with  $\delta\alpha \sim 10^{-3}$ . Comparing to our analytic results in Sec. III C, we find that the two-level approximation is quite accurate. For instance, expression (3.49) gives  $\delta\alpha \sim \Lambda \sim 10^{-3}$ , which is in good agreement with the results of numerical calculations. Further, the peak amplitude of the resonance in  $\Delta E_0$  is  $0.5$ , which agrees precisely with the numerical result in Fig. 2b.

As  $\Lambda$  increases, additional structure appears in  $\Delta E_0$ . Although Fig. 3 ( $\Lambda = 0.003$ ) appears quite similar to Fig. 2, the resonance at  $\alpha = 0.5$  is much broader, and there is a new resonance  $\alpha = 0 \pmod{1}$ . The detailed structure of these resonances is shown in Fig. 4, for slightly larger  $\Lambda$  ( $\Lambda = 10^{-2}$ ). A “double resonance” (DR) phenomenon appears

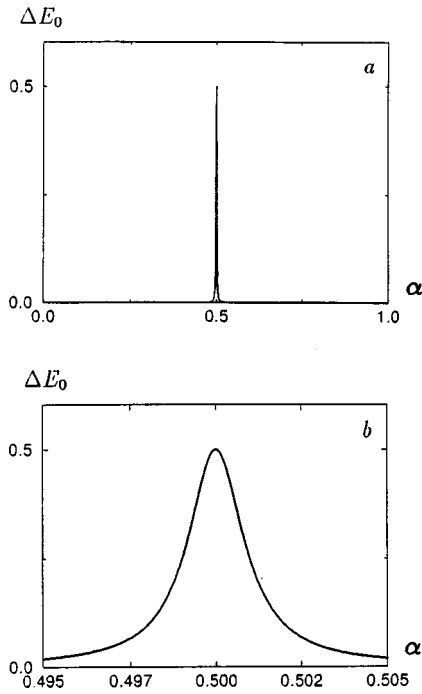


FIG. 2. Dependence of the average energy shift of the system  $\Delta E_0$  on  $\alpha$ ; (a)  $\Lambda=0.001$ ,  $\omega_0=0$ , and  $N=1$ ; (b) the same, but scaled in the vicinity of the resonant peak at  $\alpha=0.5$ .

for  $\Lambda=0.05$  and at  $\alpha=0.5$ , as shown in Fig. 5. Figure 5(a) illustrates the strong, sharp second resonance of the DR. From Fig. 5(b), we see that the second resonance also has substructure corresponding to a double peak. A similar DR phenomenon is demonstrated in Fig. 6 for  $\Lambda=0.2$ . In this case one also observes the substructure of resonances at  $\alpha=0$  [Fig. 6(c)]. A partial explanation of the results in Figs. 5 and 6 follows from Fig. 7, which shows that a greater number of levels of the unperturbed Hamiltonian contribute to the resonances shown in Fig. 6, and hence one expects a greater number of individual resonant frequencies. In particular, Fig. 7 shows that the quasienergy eigenfunction with  $\sigma=2$  actually includes four levels of the unperturbed Hamiltonian.

In Fig. 8 we indicate the dependence of  $\Delta E_0$  on  $\Lambda$  for fixed  $\omega$  and  $\alpha=0.5$  [Fig. 8(a)], and for  $\alpha=0.45$  [Fig. 8(b)]. The sharp “staircase” behavior observed at the resonant value  $\alpha=0.5$  washes out rather quickly off resonance.

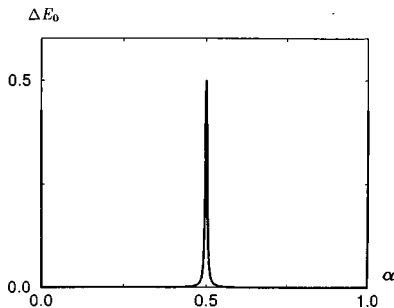


FIG. 3. Dependence of the average energy shift of the system  $\Delta E_0$  on  $\alpha$  for  $\Lambda=0.003$ ,  $\omega_0=0$ , and  $N=1$ .

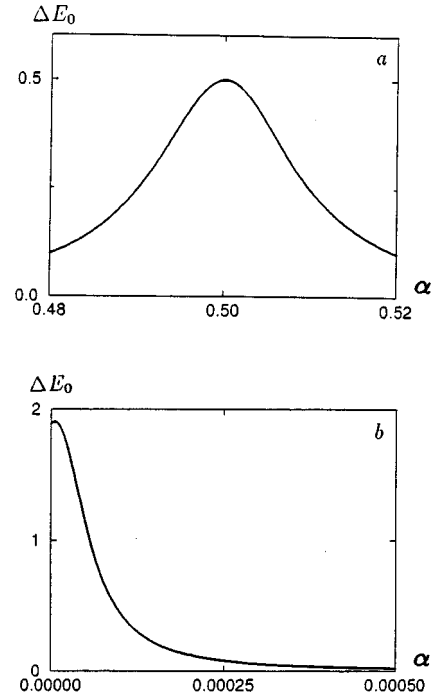


FIG. 4. Dependence of  $\Delta E_0$  on  $\alpha$  in the vicinity of  $\alpha=0.5$ ,  $\Lambda=0.01$ ,  $\omega_0=0$ , and  $N=1$  (a), and  $\alpha=0$  (b).

From our analytic results on the two-level approximation, we expect that changing the frequency of the external field changes the positions of the resonances as functions of  $\alpha$  and, in addition, modifies their shapes. This expectation is confirmed by the data shown in Fig. 9. The change in location of the resonances that occurs when parameters like  $\omega_0$  (or  $N$ ) are varied results from the changes in the value of  $\alpha$  (or  $\xi_\alpha$ ) at which the unperturbed spectrum (3.17) [or (3.58)] has degeneracies.

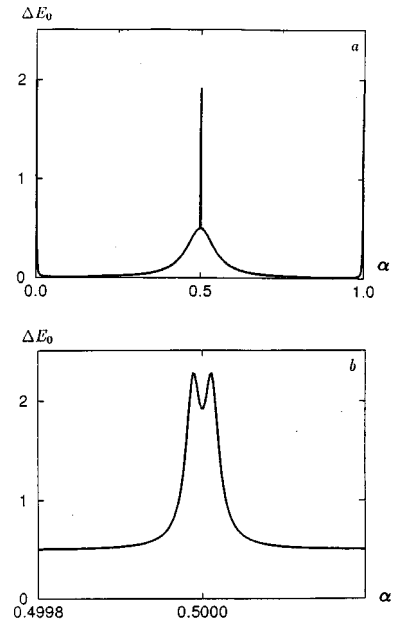


FIG. 5. Dependence of  $\Delta E_0$  on  $\alpha$ : (a)  $\Lambda=0.05$ ,  $\omega_0=0$ , and  $N=1$ ; (b) the same as in (a), but scaled in the vicinity of  $\alpha=0.5$ .

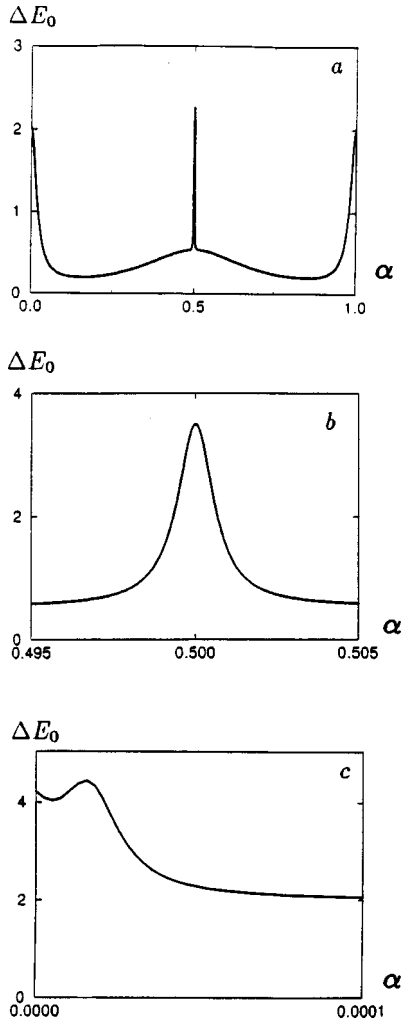


FIG. 6. Dependence of  $\Delta E_0$  on  $\alpha$ : (a)  $\Lambda=0.2$ ,  $\omega_0=0$ , and  $N=1$ ; (b) scaled in the vicinity of  $\alpha=0.5$ ; (c) scaled in the vicinity of  $\alpha=0$ .

Figure 10 demonstrates the resonant behavior of  $\Delta E_0$  as a function of flux for  $\Lambda=1$ . The characteristic quasienergy eigenfunctions involved in the resonances are shown in Fig. 11; for instance, we see that six unperturbed levels contribute to the quasienergy eigenfunction with  $\sigma=5$ . Finally, Fig. 12 demonstrates the resonant structure in the dependence  $\Delta E_0(\alpha)$  when spatial dependence of the external ac field involves the second harmonic of the angle  $\varphi$  ( $N=2$ ). In this example, the frequency of the external field  $\omega$  is detuned from resonance with the Fermi frequency  $\omega_F$  ( $\omega_0=0.2$ ). As in Fig. 9 (for the case  $N=1$ ), the resonances are shifted from the point  $\alpha=0.5$ , but they also have considerably different structure.

Thus far we have assumed that the number of electrons is odd,  $n_e=2N_e+1$ . It is possible to show that for even number of electrons,  $n_e=2N_e$ , we can still apply expression (3.42) but with the following substitution for  $\alpha$  and  $\omega_0$ :

$$\Delta E_0^{(\text{even})}(\alpha, \omega_0) = \Delta E_0^{(\text{odd})}(\alpha - 1/2, \omega_0 + 1/2). \quad (3.60)$$

Hence there is no need to present separate calculations for the case of even  $n_e$ .

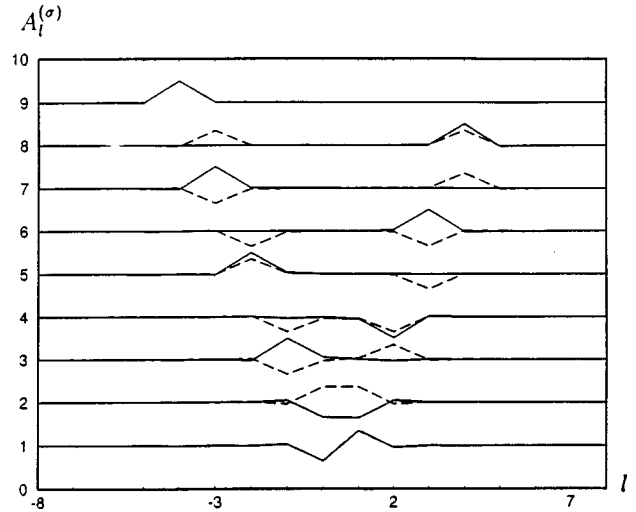


FIG. 7. Dependence of the quasienergy functions  $A_l^{(\sigma)}$  on  $l$ , for  $\sigma=1, 2, \dots, 9$ ,  $\Lambda=0.2$ ,  $\omega_0=0$ ,  $N=1$ , and  $\alpha=0.495$  (solid curve), and  $\alpha=0.5$  (dashed curve).

#### IV. INTERACTION OF TWO QUANTUM NONLINEAR RESONANCES: OVERLAP AND QUANTUM CHAOS

##### A. Effective Hamiltonian for two QNR's

When a resonant field with two frequencies ( $\omega_1$  and  $\omega_2$ ) acts on the electrons in the mesoscopic ring, two QNR's are formed. In this subsection, we derive the effective resonant Hamiltonian describing the slow dynamics of their interaction. We show that this dynamics is time dependent and, in the classical limit, corresponds to a "one-and-a-half" degree of freedom, nonintegrable system, which is expected to exhibit chaotic behavior in some regions of classical phase

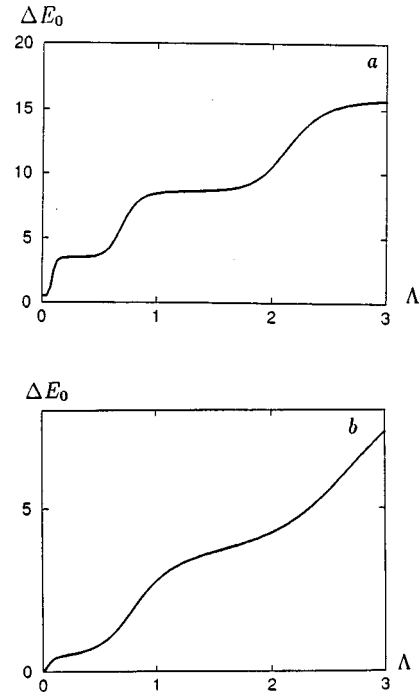


FIG. 8. Dependence of  $\Delta E_0$  on  $\Lambda$ ; (a)  $\alpha=0.5$ ,  $\omega_0=0$ , and  $N=1$ ; (b) the same as in (a), but  $\alpha=0.45$ .

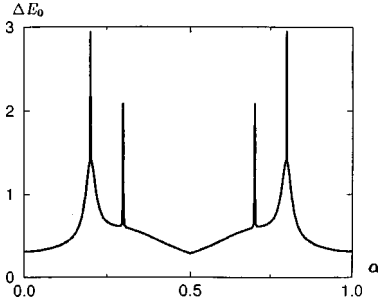


FIG. 9. Dependence of  $\Delta E_0$  on  $\alpha$ :  $\Lambda=0.2$ ,  $\omega_0=0.2$ , and  $N=1$ .

space. In the quantum problem, when QNR's interact strongly (i.e., overlap), a transition to quantum chaos can occur.

Our formulation of the effective Hamiltonian in Sec. II was deliberately chosen to be sufficiently general to include the case of two QNR's corresponding to two distinct frequencies in the resonator field. Hence we may start our explicit calculations directly from Eq. (2.28), in which the two frequencies in  $A^{\text{RES}}$  are denoted by  $\omega_1 \neq \omega_2 \neq 0$ . For simplicity, we shall take  $N=M$  in Eq. (2.28); this is possible, even though the frequencies are distinct, because of the  $z$  degree of freedom in the resonator [cf. Eq. (2.4)].

Recalling the methodology of Sec. III, we see that our task is to choose the parameter  $\nu$  in Eq. (2.23) so as to separate the fast and slow dynamics. In the present case, we choose the parameter  $\nu$  to be

$$\nu = \frac{1}{N} (\omega_1 - \Delta), \quad (4.1)$$

where  $\Delta$  is some slow frequency ( $\Delta/\omega_{1,2} \ll 1$ ) which we take to be

$$\Delta = \frac{\omega_1 - \omega_2}{2}. \quad (4.2)$$

Then the free parameter  $\nu$  is completely defined as

$$\nu = \frac{\omega_1 + \omega_2}{2N}. \quad (4.3)$$

Neglecting the high-frequency oscillating terms, from Eq. (2.28) we derive the approximate Hamiltonian

$$\begin{aligned} \hat{\mathcal{H}}_{\text{eff}} = & \sum_n [(n - n_* - \alpha)^2 + 2n_*(n - n_* - \alpha) - n\nu/\kappa] \hat{c}_l^\dagger \hat{c}_l \\ & + \frac{i}{2} \Lambda_1 e^{-i\Delta t} \sum_l \hat{c}_{l+N}^\dagger \hat{c}_l - \frac{i}{2} \Lambda_1 e^{i\Delta t} \sum_l \hat{c}_{l-N}^\dagger \hat{c}_l \\ & + \frac{i}{2} \Lambda_2 e^{i\Delta t} \sum_l \hat{c}_{l+M}^\dagger \hat{c}_l - \frac{i}{2} \Lambda_2 e^{-i\Delta t} \sum_l \hat{c}_{l-M}^\dagger \hat{c}_l, \end{aligned} \quad (4.4)$$

where  $\Lambda_{1,2} \equiv n_* \lambda_{1,2}$ . For simplicity, we assume below that  $\Lambda_1 = \Lambda_2 = \Lambda$ . We next introduce the dimensionless variables:  $\tau$  as in Eq. (3.2) and frequency

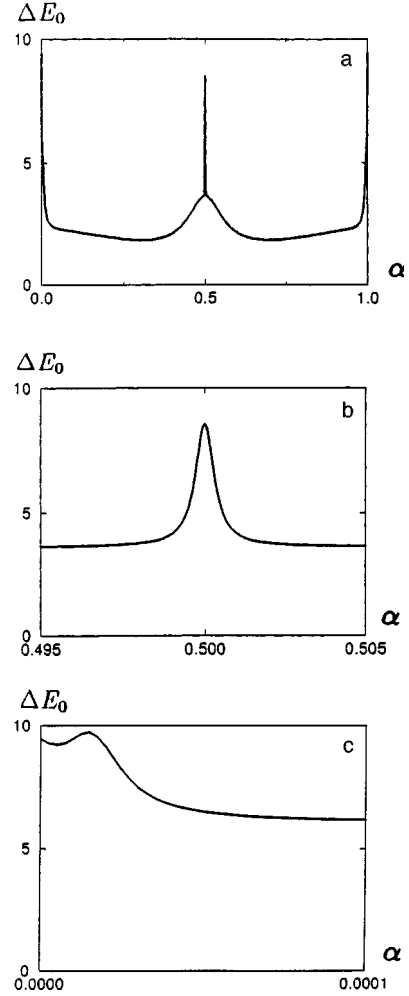


FIG. 10. Dependence of  $\Delta E_0$  on  $\alpha$ : (a)  $\Lambda=1$ ,  $\omega_0=0$ , and  $N=1$ ; (b) scaled in the vicinity of  $\alpha=0.5$ ; (c) scaled in the vicinity of  $\alpha=0$ .

$$\tilde{\Delta} = \frac{\Delta}{\kappa}. \quad (4.5)$$

As in Sec. III, focusing on the diagonal part of Eq. (4.4), neglecting irrelevant constants, and choosing  $n_*$  to be

$$n_* = \left[ \frac{(\omega_1 - \Delta)}{2N\kappa} \right]_{\text{int}}, \quad (4.6)$$

we find that the reduced Hamiltonian describing the slow dynamics of two interacting QNR's becomes

$$\begin{aligned} \hat{\mathcal{H}}_{\text{eff}} = & \sum_n (n - [(\omega_1 - \Delta)/2N\kappa]_{\text{int}} - \alpha)^2 \hat{c}_n^\dagger \hat{c}_n \\ & + i\Lambda \cos \tilde{\Delta} \tau \sum_l \hat{c}_{l+N}^\dagger \hat{c}_l - i\Lambda \cos \tilde{\Delta} \tau \sum_l \hat{c}_{l-N}^\dagger \hat{c}_l. \end{aligned} \quad (4.7)$$

The Hamiltonian  $\hat{\mathcal{H}}_{\text{eff}}$  in Eq. (4.7) can be significantly simplified by the same relabeling of states shown in Eq. (3.14). As in Sec. III, this relabeling leads to a decomposition of  $\hat{\mathcal{H}}_{\text{eff}}$  into a sum of individual terms  $\hat{\mathcal{H}}_{\text{eff}}(k)$ , with

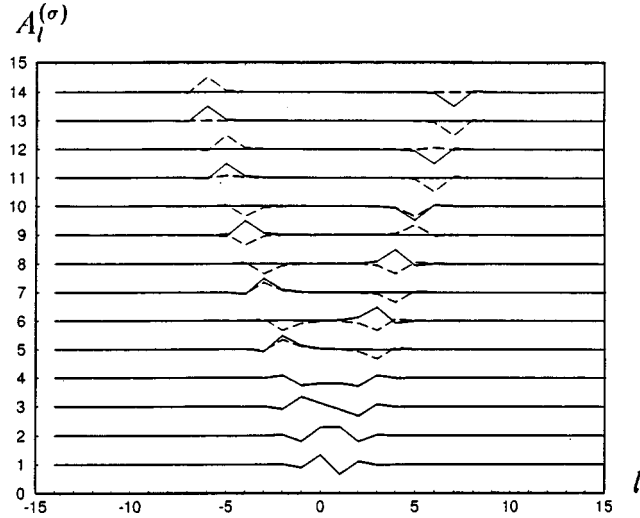


FIG. 11. Dependence of the quasienergy functions  $A_l^{(\sigma)}$  on  $l$ , for  $\sigma=1,2,\dots,14$ ,  $\Lambda=1$ ,  $\omega_0=0$ ,  $N=1$ , and  $\alpha=0.495$  (solid curve), and  $\alpha=0.5$  (dashed curve).

$$\hat{\mathcal{H}}_{\text{eff}}(k) = \sum_l \left\{ \varepsilon_{l,k} \hat{b}_l^\dagger(k) \hat{b}_l(k) + i\Lambda \cos \tilde{\Delta} \tau \sum_l \hat{b}_{l+1}^\dagger(k) \hat{b}_l(k) - i\Lambda \cos \tilde{\Delta} \tau \sum_l \hat{b}_{l-1}^\dagger(k) \hat{b}_l(k) \right\}, \quad (4.8)$$

where

$$\varepsilon_{l,k} = \{k + lN - \alpha - [(\omega_1 - \Delta)/\kappa]_{\text{int}}\}^2. \quad (4.9)$$

In distinction to the case of an isolated QNR, here the effective Hamiltonian contains explicit time dependence. Nonetheless, we can proceed exactly as in the previous case to write the operator equations for  $\hat{b}_l(k)$ , to expand the solution of this equation in terms of the operators at the initial time, and to derive equations for the dynamics of the expansion coefficients  $a_{l,l'}(\tau)$  in Eq. (3.21). We find

$$i\dot{a}_{l,l'} = \varepsilon_{l,k} a_{l,l'} + \Lambda \cos(\tilde{\Delta} \tau) a_{l-1,l'} + \Lambda \cos(\tilde{\Delta} \tau) a_{l+1,l'}, \quad (4.10)$$

with the initial conditions for equations (4.10) being the same as in Eq. (3.23).

Equations (4.10) can be written in the form (3.25a), with the resonant Hamiltonians

$$\hat{H}_r^{(k)} \left( \theta, -i \frac{\partial}{\partial \theta} \right) = \varepsilon \left( -i \frac{\partial}{\partial \theta}, k \right) + 2\Lambda \cos(\tilde{\Delta} \tau) \cos \theta, \quad (4.11)$$

$$\varepsilon \left( -i \frac{\partial}{\partial \theta}, k \right) = \left( k - i \frac{\partial}{\partial \theta} N - \alpha - [(\omega_1 - \Delta)/\kappa]_{\text{int}} \right)^2.$$

The Schrödinger equation (3.25a) with the Hamiltonians (4.11) describe the interaction of two QNR's.<sup>26–29</sup> As discussed in more detail in the Appendix, the corresponding classical Hamiltonian is time-dependent and describes a (nonintegrable) system having “one-and-a-half” degrees of freedom and hence capable of exhibiting chaos in some regions of phase space.

We can write a particular solution of Eq. (4.10) in the form

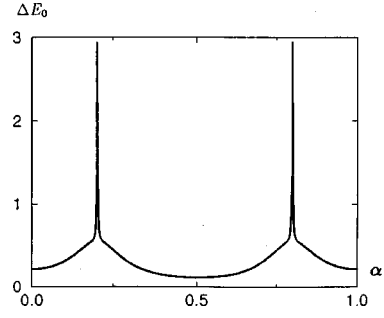


FIG. 12. Dependence of  $\Delta E_0$  on  $\alpha$ :  $\Lambda=0.2$ ,  $\omega_0=0.2$ , and  $N=2$ .

$$a_{l,l'}(\tau) = e^{-i\varepsilon_{\sigma}\tau} A_l^{(\sigma)}(\tau), \quad (4.12)$$

where  $A_l^{(\sigma)}(\tau)$  is the quasienergy eigenfunction, periodic with period  $2\pi/\tilde{\Delta}$ . The functions  $A_l^{(\sigma)}(\tau)$  provide a complete and orthogonal set of eigenfunctions. The general solution of Eq. (4.10) can be expressed as superposition of particular solutions of the form of Eq. (4.12) with time-independent coefficients  $S_{\sigma}^{(l)}$ ,

$$a_{l,l'}(\tau) = \sum_{\sigma} e^{-i\varepsilon_{\sigma}\tau} S_{\sigma}^{(l')} A_l^{(\sigma)}(\tau). \quad (4.13)$$

The difference between Eq. (4.13) and the analogous expression (3.29) for the case of an isolated QNR is that in Eq. (4.13) the eigenfunction  $A_l^{(\sigma)}(\tau)$  depends on time periodically [because the corresponding Hamiltonian (4.8) is time periodic]. Nonetheless, we have the analogs of all the expressions (3.30)–(3.33). Specifically, at  $\tau=0$  we have

$$i^{l'} \sum_{\sigma} S_{\sigma}^{(l')} A_l^{(\sigma)}(0) = \delta_{l,l'}, \quad S_{\sigma}^{(l)} = (-i)^l A_l^{(\sigma)}(0). \quad (4.14)$$

Finally, from Eqs. (3.21) and (4.14) we obtain

$$a_{l,l'}(\tau) = \sum_{\sigma} (-i)^{l'} e^{-i\varepsilon_{\sigma}\tau} A_{l'}^{(\sigma)}(0) A_l^{(\sigma)}(\tau), \quad (4.15)$$

$$\hat{b}_l(\tau, k) = \sum_{l'} i^{l'} \sum_{\sigma} (-i)^{l'} e^{-\varepsilon_{\sigma}\tau} A_{l'}^{(\sigma)*}(0) A_l^{(\sigma)}(\tau) \hat{b}_{l'}(k). \quad (4.16)$$

By analogy to the case of an isolated QNR in Eq. (3.40), we obtain the expression for the expectation value of the energy shift in the case of two interacting QNR's to be

$$\Delta E_0(\tau) \equiv \frac{1}{2Nn_*} [E(\tau) - E_0]$$

$$= \sum_{k,l} l \left\{ \sum_{\sigma,\sigma'} e^{i(\varepsilon_{\sigma} - \varepsilon_{\sigma'})\tau} A_l^{(\sigma)*}(\tau) A_l^{(\sigma')}(\tau) \right.$$

$$\times \sum_{l'} A_{l'}^{(\sigma)}(0) A_{l'}^{(\sigma')}(0) \times \langle \Psi_0 | \hat{b}_{l'}^\dagger(k) \hat{b}_{l'}(k) | \Psi_0 \rangle$$

$$\left. - \langle \Psi_0 | \hat{b}_l^\dagger(k) \hat{b}_l(k) | \Psi_0 \rangle \right\}. \quad (4.17)$$

As before, we denote the time average of  $\Delta E_0(\tau)$  by  $\Delta E_0$ .

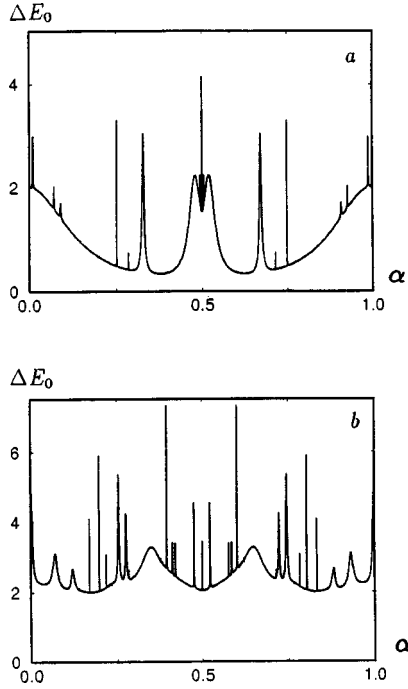


FIG. 13. Dependence of  $\Delta E_0$  on  $\alpha$  for two interacting QNR's: (a)  $\Lambda=0.4$ ,  $\Delta=1$ ,  $\Omega=0$ , and  $N=1$ ; (b) the same as in (a), but  $\Lambda=1$ .

#### B. Numerical study of average energy shift for two QNR's

Our numerical results for two interacting QNR's are summarized in Figs. 13–15. As in the case of an isolated QNR, we assume that the number of electrons is odd,  $n_e = 2N_e + 1$ . Also, in the numerical calculations we have chosen  $\omega_F = (\omega_1 + \omega_2)/2$ . Figures 13(a) and 13(b) demonstrate the dependence of  $\Delta E_0$  on the AB flux  $\alpha$  for a rather large amplitudes of the ac field:  $\Lambda=0.4$  in Fig. 13(a) and  $\Lambda=1$  in Fig. 13(b). The resonance structure is highly complicated in these cases, and reflects the significant modifications in the structure of the quasienergy eigenfunctions when  $\alpha$  is varied. Figures 14 and 15 illustrate the modifications to the quasienergy eigenfunctions as  $\alpha$  is varied from a nonresonant value

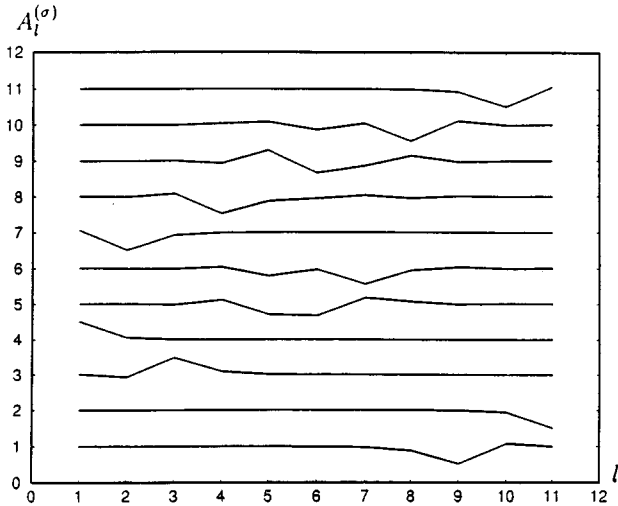


FIG. 14. Dependence of the quasienergy functions  $A_l^{(\sigma)}$  on  $l$ , for  $\sigma=1,2,\dots,11$ ,  $\Lambda=1$ ,  $\Delta=1$ ,  $\Omega=0$ ,  $N=1$ , and  $\alpha=0.2614$ .

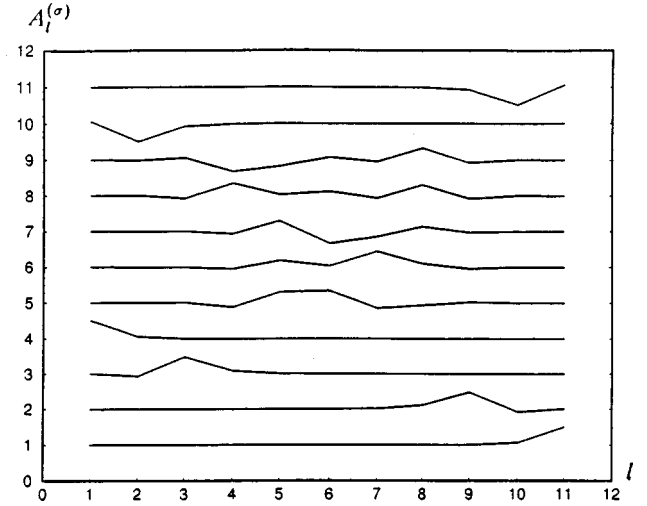


FIG. 15. Dependence of the quasienergy functions  $A_l^{(\sigma)}$  on  $l$ , for  $\sigma=1,2,\dots,11$ ,  $\Lambda=1$ ,  $\Delta=1$ ,  $\Omega=0$ ,  $N=1$ , and  $\alpha=0.254\ 67$  (resonant value).

$\alpha=0.2614$  (shown in Fig. 14) to a resonant one,  $\alpha=0.25467$  (shown in Fig. 15). In the resonant case, seven unperturbed levels contribute to the structure of the eigenfunction with  $\sigma=8$ . This effect can be interpreted as a “delocalization” of the quasienergy eigenfunctions in the system when two QNR's strongly interact. Usually, problems connected with a delocalization of the quasienergy eigenfunctions at the transition to quantum chaos are investigated in the quasiclassical region of parameters ( $\delta n \gg 1$ ).<sup>28,29,41,42</sup> In our numerical calculations, we have chosen  $\Lambda$  in the intermediate range ( $\Lambda \lesssim 3$ ). For these values of  $\Lambda$ , the characteristic number of levels,  $\delta n \lesssim 10$ . In this region, the problem of delocalization of the quasienergy eigenfunctions at the transition to quantum chaos has not been developed. Note that the formal limitation on the parameter  $\Lambda$ , which follows from the condition  $\lambda_{1,2} \leq n_F$ , is  $\Lambda \leq n_F^2$ , which is easily satisfied.

#### V. DISCUSSION AND CONCLUSION

We have established that the problem of AB oscillations in a mesoscopic ballistic ring threaded by both a constant magnetic flux and a time-dependent resonant magnetic field can be studied using the concept of “quantum nonlinear resonance” (QNR), provided that the frequency of the ac field,  $\omega$ , satisfies  $\omega \approx \omega_F$ , where  $\omega_F$  is the frequency corresponding to transitions in the vicinity of the Fermi level,  $n_F$ .

QNR is characterized by the number of levels,  $\delta n$ , of the unperturbed Hamiltonian involved in the dynamics. Our numerical calculations show that even for  $\Lambda = \lambda n_F \lesssim 1$ , the “widest” quasienergy eigenfunctions involve in their structure (and hence in the electron dynamics) a fairly small number of levels of the unperturbed Hamiltonian,  $\delta n \lesssim 5$ . For an external field with a single frequency, we derived a Schrödinger equation describing the slow dynamics of an isolated QNR, and showed that it corresponded to a system with one degree of freedom, whose classical and quantum dynamics are integrable and thus everywhere regular. When the ac field includes two frequencies which satisfy the condition  $\omega_{1,2} \sim \omega_F$ , two QNR's occur, and a transition to quantum chaos

can take place. In the limit  $\Lambda \leq 1$ , the number of levels involved in the electrons dynamics is of order  $\delta n \leq 10$ . The effective Hamiltonian describing two interacting QNR's is time periodic, and corresponds to the system with 1.5 degrees of freedom. This system is nonintegrable, and, in the classical limit, its dynamics is generally chaotic. Thus mesoscopic semiconducting rings in time-dependent external fields provide an interesting solid-state system, quite distinct from the widely studied Rydberg atoms,<sup>31–37</sup> in which to study quantum chaos.

For both cases, that of an isolated QNR, and that for two interacting QNR's, we calculated numerically the dependence of the ground-state energy shift  $\Delta E_0(\alpha, \Lambda)$  on the dimensionless magnetic flux  $\alpha$ , and on the amplitude ( $\Lambda$ ) of the ac magnetic field. The dependence  $\Delta E_0$  on  $\alpha$  is periodic with the period 1 (as it should be from the general considerations<sup>43</sup>) and shows a characteristic resonant behavior.

For  $\Lambda \ll 1$ , the two-level approximation allowed us to estimate analytically the shape of the resonance and its location. In this case, the width of the resonance is  $\delta\alpha \sim \Lambda$ . The resonances in the dependence  $\Delta E_0(\alpha, \Lambda)$  are located at the values  $\alpha_r$ , where the quasidegeneracy of the unperturbed spectrum of the Hamiltonian describing the slow dynamics takes place. Numerical calculations show that in the vicinity of these points  $\alpha_r$ , a significant modification of the quasienery eigenfunctions occurs. The resonance positions  $\alpha_r$  depend linearly on the value of the frequency detuning,  $\omega_0 = \omega - \omega_F$ , from the exact resonance ( $\omega_0 = 0$ ). Thus, this dependence can be a subject for the experimental observations. The staircase dependence of  $\Delta E_0$  on  $\Lambda$  shown in Fig. 8, also could be observed in experiments.

Our results extend previous studies of AB phenomena in time-dependent fields. For purposes of comparison, we note that in Ref. 19, this general problem was investigated using a high-frequency (nonresonant) electromagnetic field with a frequency  $\omega \gg T_0/\hbar$ . In this case, the influence of the external field is reduced to the appearance of an additional periodic effective potential in the electron Hamiltonian, which slightly modifies the energy spectrum. The amplitude of the AB oscillations either remains effectively constant or practically vanishes (indicating dielectric behavior) if the Fermi level falls inside the forbidden miniband. Reference 18, studied the low-frequency limit of the conductance in a metallic ring influenced by an ac field, and showed that here the conductance is sensitive mainly to the static part of the magnetic flux. Two previous works<sup>11,21</sup> discussed possible resonant AB effects in metallic mesoscopic rings in ac fields, the first examining the influence of the resonant absorption of a circular ac electric field on conductance oscillations,<sup>11</sup> and the second treating resonant oscillations of the absorbed energy.<sup>21</sup> These studies also found the resonance peaks in the amplitude of AB oscillations. However, the perturbative methods exploited in their analytical calculations did not permit them to look into the most interesting case when the nonlinear effects play a significant role, and in particular they did not discuss the possibility of quantum chaos.

To clarify the differences and similarities between QNR's and the quantum chaos expected in our present "solid-state atoms" (Ref. 17) and the more familiar Rydberg atom case,<sup>31–37</sup> we should recall that for the microwave ionization

of highly excited atoms QNR's have the following characteristics.

(i) The motion of an excited electron in a hydrogen atom takes place in the quasiclassical region ( $n_0 \gg 1$ ). Because the unperturbed quantum energy spectrum is of the form  $-1/2n^2$ , the corresponding nonlinear classical dynamics is characterized by particular dependence of the frequency  $\Omega$  on the action  $I = \hbar n$  (energy) of the form  $\Omega = \Omega(I) = 1/I^3$ .

(ii) The external microwave field  $F \cos \omega_0 t$ , with  $\omega_0 \sim 10$  GHz, creates a series of primary resonances  $n\Omega(I_n) = \omega_0$  at  $I_n = (n/\omega_0)^{1/3}$ . Thus a single frequency creates several resonances. These resonances are nonlinear, which leads to their saturation under the action of the external microwave resonant field.

(iii) Below the critical amplitude of the external field,  $F < F_{cr}$ , the resonances can be considered as isolated. Under the condition  $F > F_{cr}$ , the resonances strongly interact, and the transition to the dynamical chaos takes place.

For the mesoscopic ring problem, the unperturbed energy spectrum has the form  $E_n \sim (n - \alpha)^2$ . Consequently, the nonlinear dependence of the frequency of electron's oscillation is  $\Omega(I) \sim I$ . In this case, an external field with a single frequency creates a single QNR, so the dynamics remains regular. To create two (or more) primary nonlinear resonances we need to apply an external field with two (or more) distinct frequencies  $\omega_1$  and  $\omega_2$ , both in the range  $\omega_F$ , which for our systems is roughly  $\omega_F \sim \nu_F/R \sim 1 - 100$  GHz. In this case can we have resonance overlap and the transition to quantum chaos.

Concerning experimental confirmation of the effects we have predicted, it is important to note that initial experiments involving electrons in semiconducting mesoscopic rings coupled to an electromagnetic resonator have very recently been reported.<sup>44</sup> Although the experimental configuration and details in that study are not appropriate for direct comparison, nevertheless the work does indicate promising prospects for a such a comparison in the near future. For the experimental parameters discussed in Sec. II— $R = 10^{-4}$  cm,  $r_0 = 0.1$  cm,  $n_F = 10^2 - 10^3$ ,  $k'_{nr} \sim 2$ , and  $H_{cr} = 2.5 - 25$  Oe—and for  $\Lambda \leq 1$ , we find that the magnitude of the resonance peaks in the average energy shift is

$$\Delta E_0 \sim 10^{-4} - 10^{-3} \text{ eV}, \quad (5.1)$$

which we believe will be detectable given the proper experimental configuration.

To conclude, let us mention a number of interesting open questions that merit further investigation. One obvious important theoretical issue is the effect of electron-electron interactions on the nonlinear phenomena investigated here. Also, if the semiconductor ring is off centered in the cavity, then the perturbation terms in Eq. (2.10) should be modified for some periodic functions in  $\varphi$ . In this case, one still should expect the resonant transitions initiated by the resonant cavity field. But the matrix elements of these transitions will be different from those used in this paper. As a result, one should not expect some qualitative modifications of the results discussed in this paper. At the same time, to investigate quantitatively the location of the modified resonances, one needs to perform additional analytical and numerical investigations. We are currently studying this question, within the

framework of the Luttinger-liquid model. Modifications of our considerations to multichannel semiconductor and metallic mesoscopic systems (by including effects of dissipation and of many channels) are also of interest. The inclusion of impurities and a self-consistent magnetic field is also of interest, in view of recent studies<sup>39</sup> showing that AB oscillations can lead to the appearance of additional fluctuations of current in ultrasmall devices. Finally, the possibility that the resonance phenomena we predict might be useful for detection of very weak magnetic radiation signal is also worthy of further study.

### ACKNOWLEDGMENTS

We are grateful to Boris Al'tshuler, David Ferry, and Mark Sherwin for useful discussions. E.N.B. and I.V.K. thank the Los Alamos National Laboratory and the Department of Physics at the University of Illinois at Urbana-Champaign for hospitality. This work was partially supported by Grant No. 94-02-04410 of the Russian Fund for Basic Research and by Linkage Grant No. 93-1602 from the NATO Special Programme Panel on Nanotechnology. Work at Los Alamos was partly supported by the Defense Advanced Research Projects Agency.

### APPENDIX: CLASSICAL AND QUANTUM NONLINEAR RESONANCES

#### Summary of nonlinear resonance

The concept of “nonlinear resonance” plays a crucial role in our understanding of Hamiltonian chaos in classical mechanics (see, e.g., Ref. 45 for a clear introduction). In an integrable classical system, the entire phase space is foliated by invariant tori, and the motion is regular everywhere. Although all one degree of freedom Hamiltonian systems are completely integrable, higher degree of freedom integrable systems are rare, and are isolated in the sense that a generic perturbation around such a system destroys the integrability. The Kolmogorov-Arnold-Moser (KAM) theorem proves that, for a generic perturbation of an integrable, nonlinear (i.e., nonharmonic) system some (“nonresonant”) tori remain, so that there are still regions of regular motion. But many “resonant” tori are destroyed and their images in the Poincaré sections are replaced by chaotic trajectories. The center of a “nonlinear resonance” (henceforth, NR) is one of the elliptic points arising from the destruction of a resonant torus. Around this elliptic point, there are stable oscillations corresponding to the “slow” dynamics referred to in the text. Importantly, for an isolated NR, the slow dynamics correspond to the dynamics of a single degree of freedom and hence are (locally) integrable. In a general, there are many NR's in a perturbed integrable system. When there are two nearby but separated NR's, each of them acts as a fast—and hence irrelevant and/or nonresonant—perturbation on the other, but, when they overlap in phase space, the two slow dynamics become strongly coupled, and one has the “Chirikov overlap criterion” for (global) chaos.<sup>45,46</sup>

The extension of these ideas to quantum mechanics was first described in Ref. 25, in which the theory of QNR was developed to describe the influence of a resonant external field on a quantum system with a nonequidistant spectrum

(corresponding to the assumption of anharmonicity in the classical analog). The main parameters characterizing a QNR are the number of quasienergy levels  $\delta n$  involved in the resonance (the value  $\delta n$  also characterizes the number of levels of the unperturbed Hamiltonian involved in the dynamics), and the characteristic frequency of slow oscillations (phase oscillations),  $\Omega_{\text{ph}}$ . QNR is perhaps mostly readily understood in the quasiclassical regime, which corresponds to large amplitude  $\Lambda$  of the external ac field. For example, this regime be realized in a region of parameters of a so-called “moderate nonlinearity,”<sup>45,46</sup>  $\Lambda \ll \gamma \ll 1/\Lambda$ , where  $\gamma$  is a dimensionless parameter describing the strength of the nonlinearity (or anharmonicity) in the spectrum (e.g.,  $\gamma \sim |n_r E''_{n_r}/E_{n_r}|$ , where  $E''_{n_r}$  is the second derivative of the energy with respect to level number. In this case, the following conditions are satisfied:  $\Omega_{\text{ph}} \sim \sqrt{\Lambda} \gamma \omega \ll \omega$ ,  $\delta n \sim \sqrt{\Lambda/\gamma} \gg 1$ ,  $\delta n/n_r \ll 1$ , where  $n_r$  is a characteristic resonant level. In this region of parameters, QNR is the direct quantum analog of the classical (NR) described above.

However, QNR is a very general phenomenon in quantum-dynamical systems with nonequidistant energy spectra,<sup>26–29,36</sup> and indeed also occurs in the strongly quantum limit, which in our present study corresponds to rather small amplitude  $\Lambda$  of the external ac resonant field. In this case, QNR reduces to the problem of a few-level quantum system influenced by ac resonant external field. For sufficiently small amplitude  $\Lambda$ , QNR reduces to a two-level system in a resonant field. Then the characteristic frequency of small oscillations  $\Omega_{\text{ph}} = \Omega_R \propto \Lambda$ , where  $\Omega_R$  is the Rabi frequency (see, e.g., Ref. 47). Thus as  $\Lambda$  decreases, there is a crossover in the behavior of  $\Omega_{\text{ph}}(\Lambda)$  and  $\delta n(\Lambda)$ .<sup>37</sup> In the general situation, the number of levels involved in the QNR dynamics is typically of intermediate size ( $\delta n \lesssim 10$ ), and is too small for the system to be considered quasiclassical (see, for example, Refs. 28 and 37) but too large for the strongly quantum, few-level limit to apply. In this “intermediate quantum system” regime, which, as we have seen, applies to the systems we have considered in this paper, one must generally resort to numerical studies to solve the QNR problem.

#### Classical analogs of QNR effective Hamiltonians

The effective Hamiltonian for isolated QNR given by Eq. (3.25b) has a formal classical analog, which helps clarify the dynamics. Using standard arguments, we introduce the dimensionless classical action  $I$  by the substitution

$$-i \frac{\partial}{\partial \theta} \rightarrow \alpha \rightarrow I, \quad (\text{A1})$$

from which it follows immediately that Eq. (3.25b) corresponds to the classical Hamiltonian

$$H_r^{(k)}(\theta, I) = (k + NI - n_*)^2 + \left( 2n_* - \frac{\omega}{N\kappa} \right) (k + NI - n_*) + \Lambda \cos \theta. \quad (\text{A2})$$

In Eq. (A2) the index  $k$  corresponds to the classical action  $k \rightarrow \hbar k = I_k$ , which is a continuous parameter varying in the region  $I_k \in [\hbar n_0, \hbar(n_0 + N - 1)]$ . The expression in Eq. (A2) has the standard form of the Hamiltonian of classical nonlin-



ear resonance,<sup>45,46</sup> and describes the slow resonant dynamics of the classical equivalent of system (2.1), when the external ac field has one resonant frequency  $\omega \approx \omega_F$ . The corresponding classical dynamics can be studied using Hamilton's equations  $\dot{\theta} = \partial H_r^{(k)} / \partial I$ ,  $\dot{I} = -\partial H_r^{(k)} / \partial \theta$ . Since Hamiltonian (A2) is time independent and describes a system with one degree of freedom, the classical dynamical system is integrable in this case, and the dynamics is everywhere regular.<sup>45,46</sup>

In the case of two QNR's, the corresponding classical Hamiltonian is time-periodic and assumes the form

$$H_r^{(k)}(\theta, I) = (k + IN - [(\omega_1 - \Delta)/\kappa]_{\text{int}})^2 + 2\Lambda \cos(\tilde{\Delta}\tau) \cos\theta, \quad (\text{A3})$$

where the index  $k$  can take continuous values as discussed above. The dynamical system described by the Hamiltonian (A3) has one-and-a-half degrees of freedom,<sup>45,46</sup> and is non-integrable. In this case, the classical dynamics exhibits chaos in some regions of phase space. The corresponding quantum dynamics gives an example of quantum chaos. Specific physical examples of such systems, apart from the one considered in this paper, can be found in Refs. 28, 29, 36, 42, 45, and 46 (see also references therein).

- <sup>1</sup>Y. Aharonov and D. Bohm, Phys. Rev. **115**, 485 (1959).
- <sup>2</sup>S. Washburn and R. A. Webb, Adv. Phys. **35**, 375 (1986).
- <sup>3</sup>M. Büttiker, Y. Imry, and R. Landauer, Phys. Rev. A **96**, 365 (1983).
- <sup>4</sup>I. O. Kulik, Pis'ma Zh. Eksp. Teor. Fiz. **11**, 407 (1970) [JETP Lett. **11**, 275 (1970)].
- <sup>5</sup>Y. Imry, in *Directions in Condensed Matter Physics*, edited by G. Grinstein and G. Mazenko (World Scientific, Singapore, 1986), p. 101.
- <sup>6</sup>H.-F. Cheung, Y. Gefen, E. K. Riedel, and W.-H. Shih, Phys. Rev. B **37**, 6050 (1988).
- <sup>7</sup>L. P. Lévy, G. Dolan, J. Dunsmuir, and H. Bouchiat, Phys. Rev. Lett. **64**, 2074 (1990).
- <sup>8</sup>V. Chandrasekhar *et al.*, Phys. Rev. Lett. **67**, 3578 (1991).
- <sup>9</sup>D. Mailly, C. Chapelier, and A. Benoit, Phys. Rev. Lett. **70**, 2020 (1993).
- <sup>10</sup>B. Altshuler, in *Nanostructures and Mesoscopic Systems*, edited by W. P. Kirk and M. A. Reed (Academic, New York, 1992).
- <sup>11</sup>I. E. Aronov, I. V. Krive, R. I. Shekhter, and M. Jonson, Low Temp. Phys. **19**, 668 (1993).
- <sup>12</sup>M. Büttiker and R. Landauer, Phys. Rev. Lett. **49**, 1739 (1982).
- <sup>13</sup>D. L. Haavig and R. Reifenberger, Phys. Rev. B **26**, 6408 (1982).
- <sup>14</sup>A. D. Stone, M. Ya. Azbel, and P. A. Lee, Phys. Rev. B **31**, 1707 (1985).
- <sup>15</sup>A.-P. Jauho and M. Jonson, Superlattices Microstruct. **6**, 303 (1989).
- <sup>16</sup>M. Wagner, Phys. Rev. B **49**, 16 544 (1994).
- <sup>17</sup>M. S. Sherwin, in *Quantum Chaos*, edited by G. Casati and B. V. Chirikiv (Cambridge University Press, Cambridge, 1995), p. 209.
- <sup>18</sup>M. Büttiker, Phys. Rev. B **32**, 1846 (1985).
- <sup>19</sup>I. E. Aronov, E. N. Bogachev, and I. V. Krive, Phys. Lett. A **164**, 331 (1992).
- <sup>20</sup>I. E. Aronov, A. Grincwajg, M. Jonson, R. I. Shekhter, and E. N. Bogachev, Solid State Commun. **91**, 75 (1994).
- <sup>21</sup>G. M. Genkin and G. A. Vugalter, Phys. Lett. A **189**, 415 (1994).
- <sup>22</sup>V. E. Kravtsov, Phys. Lett. A **172**, 452 (1993).
- <sup>23</sup>V. E. Kravtsov and V. I. Yudson, Phys. Rev. Lett. **70**, 210 (1993).
- <sup>24</sup>I. Golhirsch, D. Lubin, and Y. Gefen, Phys. Rev. Lett. **67**, 3582 (1991); Y. Gefen, D. Lubin, and I. Golhirsch, Phys. Rev. B **46**, 7691 (1992); D. Lubin and I. Golhirsch, *ibid.* **46**, 2617 (1992); D. Lubin, *ibid.* **46**, 4775 (1992).
- <sup>25</sup>G. P. Berman and G. M. Zaslavsky, Phys. Lett. A **61**, 295 (1977).
- <sup>26</sup>G. P. Berman, G. M. Zaslavsky, and A. R. Kolovsky, Zh. Eksp. Teor. Fiz. **81**, 506 (1981) [Sov. Phys. JETP **54**, 272 (1981)].
- <sup>27</sup>G. P. Berman, *Quantum Chaos of Interacting Nonlinear Resonances, CHAOS, Soviet-American Perspectives on Nonlinear Science*, edited by D. K. Campbell (AIP, New York, 1990).
- <sup>28</sup>G. P. Berman and A. R. Kolovsky, Usp. Fiz. Nauk **162**, 95 (1992) [Sov. Phys. Usp. **35**, 303 (1992)].
- <sup>29</sup>G. P. Berman, O. F. Vlasova, and F. M. Izrailev, Zh. Eksp. Teor. Fiz. **93**, 470 (1987) [Sov. Phys. JETP **66**, 269 (1987)].
- <sup>30</sup>G. Casati, B. V. Chirikov, D. L. Shepelynsky, and I. Guarneri, Phys. Rep. **154**, 77 (1987).
- <sup>31</sup>J. E. Bayfield and P. M. Koch, Phys. Rev. Lett. **33**, 258 (1974).
- <sup>32</sup>J. E. Bayfield, S.-Y. Luie, L. C. Perotti, and M. P. Skrzypkowski, Physica D **83**, 46 (1995).
- <sup>33</sup>J. E. Bayfield, S.-Y. Luie, L. C. Perotti, and M. P. Skrzypkowski, Phys. Rev. A **53**, R12 (1996).
- <sup>34</sup>P. M. Koch, Physica D **83**, 178 (1994).
- <sup>35</sup>P. M. Koch and K. A. H. van Leeuwen, Phys. Rep. **255**, 289 (1995).
- <sup>36</sup>L. E. Reichl, *The Transition to Chaos in Conservative Classical Systems: Quantum Manifestations* (Springer-Verlag, Berlin, 1992).
- <sup>37</sup>G. P. Berman, E. N. Bulgakov, and D. D. Holm, Physica D **83**, 55 (1995).
- <sup>38</sup>J. D. Jackson, *Classical Electrodynamics* (John Wiley, New York, 1975).
- <sup>39</sup>D. K. Ferry, Y. Takagaki, and J.-R. Zhou, Jpn. J. Appl. Phys. **33**, 873 (1994).
- <sup>40</sup>J.-R. Zhou and D. K. Ferry, IEEE Trans. Electron Devices **39**, 473 (1992).
- <sup>41</sup>F. M. Izrailev, Phys. Rep. **196**, 299 (1990).
- <sup>42</sup>G. Casati and B. V. Chirikov, in *Quantum Chaos* (Ref. 17), p. 3.
- <sup>43</sup>N. Byers and C. N. Yang, Phys. Rev. Lett. **7**, 46 (1961).
- <sup>44</sup>B. Reulet, M. Ramin, H. Bouchiat, and D. Mailly, Phys. Rev. Lett. **75**, 124 (1995).
- <sup>45</sup>B. V. Chirikov, Phys. Rep. **52**, 263 (1979).
- <sup>46</sup>A. J. Lichtenberg and M. A. Leiberman, *Regular and Stochastic Motion* (Springer-Verlag, New York, 1983).
- <sup>47</sup>L. D. Landau and E. M. Lifshitz, *Quantum Mechanics* (Pergamon, Oxford, 1977).